



Implications of new geochronological constraints on the Aberfeldy stratiform barite deposits, Scotland, for the depositional continuity and global correlation of the Neoproterozoic Dalradian Supergroup

N.R. Moles^{a,*}, D. Selby^b

^a School of Applied Sciences, University of Brighton, Cockcroft Building, Lewes Road, Brighton BN2 4GJ, UK

^b Department of Earth Sciences, Durham University, Durham DH1 3LE, UK

ARTICLE INFO

Keywords:

Neoproterozoic
Dalradian Supergroup
Marinoan and Sturtian panglaciations
Global Boundary Stratotype Section and Point for the Tonian-Cryogenian boundary
Re-Os geochronology
Aberfeldy stratiform barite deposits

ABSTRACT

The Dalradian Supergroup of largely clastic metasediments in Scotland and Ireland is a well-known record of Neoproterozoic to Cambrian sedimentation on the Laurentian margin. Its apparent long duration, from ~ 800 to ~ 500 Ma, has encouraged a search for tectonic breaks and unconformities within the sequence. One suggestion is that a break in sedimentation occurred within the upper part of the Argyll Group, specifically in the Easdale Subgroup. Here we report dates for demonstrably synsedimentary barite mineralization hosted by the Easdale Subgroup Ben Eagach Schist Formation. Bedded pyrite from the Foss and the Ben Eagach–Duntanlich barite deposits, stratigraphically < 100 m apart, yields Re-Os ages of 604.0 ± 7.2 Ma and 612.1 ± 18.6 Ma respectively with two-sigma overlap. These ages are similar to the previously constrained 601 ± 4 Ma Tayvallich Volcanic Formation lying 2–5 km stratigraphically above. The new ages suggest continuous sedimentation through this period and, in combination with existing time markers, increase the likelihood that the basal-Argyll, Port Askaig Formation diamictite represents the Marinoan glaciation rather than the Sturtian glacial episode which may not be represented in the Dalradian sequence. As such, we urge caution in using the Dalradian in global compilations of Neoproterozoic history until further geochronological constraints are obtained for the Cryogenian-Tonian parts of the stratigraphy, which is now a high priority.

1. Introduction

The Dalradian Supergroup in Scotland (UK) and northwest Ireland is an internationally important clastic sedimentary sequence, cumulatively ~ 25 km thick, through the Neoproterozoic to basal Cambrian (Pringle, 1940; Dalziel and Soper, 2001; Dempster et al., 2002; Rooney et al., 2011). As with other remnants of Laurentia, such as the North American Cordilleran margin (Yonkee et al., 2014), the Dalradian Supergroup comprises multiple tectonostratigraphic units that record the evolution of the breakup of the Rodinia supercontinent from early extension to subsequent rifting, magmatism and development of a continental passive margin. Carbon, sulfur and strontium chemostratigraphic profiles of Dalradian strata are used in global correlations of the Tonian-Cryogenian-Ediacaran succession (e.g. Brasier and Shields, 2000; Shields-Zhou et al., 2016; Hoffman et al., 2017). Recently, a Dalradian locality in Scotland has been proposed as a Global Boundary Stratotype Section and Point for the Tonian-Cryogenian boundary

(Fairchild et al., 2018).

However, in comparison with carbonate-dominated Neoproterozoic successions such as those in China, a major disadvantage of the Dalradian and North American Cordilleran sequences is that existing time markers are scarce, indeed, ‘frustratingly sparse’ according to Prave and Fallick (2011). This paucity of datable materials is due to regional metamorphism and to the limited stratigraphic range of carbonates. In the Dalradian, reliable geochronological constraints from fossil evidence are present only in the topmost strata (upper Southern Highland Group) deposited in the Cambrian. Key time markers are provided by U-Pb dating (Fig. 2a) of one volcanic unit, the Tayvallich Volcanic Formation (Halliday et al., 1989; Dempster et al., 2002) and of pegmatite in basement rocks (Noble et al., 1996) which suggests that sedimentation is younger than 806 Ma (Strachan et al., 2002).

A further problem with the paucity of reliable time markers is that significant time gaps may be hidden in the succession. The apparent long duration of deposition of the Dalradian Supergroup, spanning some 350

* Corresponding author.

E-mail address: n.moles@brighton.ac.uk (N.R. Moles).

<https://doi.org/10.1016/j.precamres.2022.106925>

Received 28 July 2022; Received in revised form 21 November 2022; Accepted 23 November 2022

Available online 12 December 2022

0301-9268/© 2022 The Author(s). Published by Elsevier B.V. This is an open access article under the CC BY license (<http://creativecommons.org/licenses/by/4.0/>).

Ma (from ~ 820 to 468 Ma according to Tanner, 1995) appears incompatible with the Wilson Cycle (Woodcock, 2004) and this has encouraged a search for tectonic breaks and unconformities. These are difficult to discern due to lateral facies and thickness changes, scarcity of marker beds, orogenic thrust-fault reactivation of pre-orogenic extensional faults ('slides'), and syn- to post-orogenic intrusion of huge volumes of magma (Fig. 1a). During rifting of Rodinia, sedimentary basins were interspersed with sediment-starved areas, expressed locally as stratigraphic omissions and overstep of subsequent formations (Stephenson et al., 2013). One suggestion (by Dempster et al., 2002) that we discuss later is that a break in sedimentation occurred within the upper part of the Argyll Group (Fig. 1a), specifically in the Easdale Subgroup (Fig. 2a), at around 600 Ma.

Here we present evidence that pyrite within bedded barite-sulfide mineralization comprising the Aberfeldy deposits is synsedimentary or very early diagenetic in origin, and report new pyrite Rhenium-Osmium analyses. We discuss how the Re-Os dates provide further constraints on the stratigraphic position and timing of putative tectonic breaks and of glaciogenic sediments in the Dalradian Supergroup.

The stratiform mineralization is hosted within the Easdale Subgroup by the Ben Eagach Schist Formation (Fig. 2b) which can be traced continuously for ~ 200 km from Easdale in the SW Highlands through the central Grampian Highlands to NE Scotland (Fig. 1a). Graphitic pelites of the Easdale Slate overlain by calcareous phyllites in the southwest of Scotland are correlated with the Ben Eagach Schist and Ben Lawers Schist respectively in the Aberfeldy area in Perthshire (Perth and Kinross District) in the central Grampian Highlands (Fig. 1b) (Harris et al., 1994; Stephenson and Gould, 1995; Stephenson et al., 2013; Treagus et al., 2013). Pyrite Re-Os dates have been obtained separately for two discrete stratiform barite deposits, Foss and Ben Eagach-Duntanlich, that are hosted within upper and lower levels respectively of the ~ 300 m thick Ben Eagach Schist Formation (Fig. 1b, 2b).

In addition to geochronology, pyrite Re-Os data also constrain the mode of formation of the stratiform barite deposits. The traditional sedimentary exhalative ('sedex') model for bedded barite and Zn-Pb sulfides, involving seabed precipitation of chemical sediments (e.g. Emsbo et al., 2016), is currently contentious with some authors arguing for an entirely diagenetic origin (e.g. Magnall et al., 2020). Due to this genetic uncertainty the deposit type has been renamed 'clastic-dominant Zn-Pb-barite deposits' (Leach et al., 2010). Multiple dates and/or a non-isochronous $^{187}\text{Re}/^{188}\text{Os}$ - $^{187}\text{Os}/^{188}\text{Os}$ dataset would lend support to a post-depositional replacive model, whereas a positive correlation between $^{187}\text{Re}/^{188}\text{Os}$ and $^{187}\text{Os}/^{188}\text{Os}$ and relatively uniform initial $^{187}\text{Os}/^{188}\text{Os}$ compositions would support a syngenetic model involving large volumes of hydrothermal fluid circulating through the underlying sediment pile and/or continental basement.

2. The Aberfeldy barite deposits

The Aberfeldy deposits, located in upland moors north of the town of Aberfeldy (Fig. 1), comprise the largest UK resource of the industrial mineral barite (Treagus, 2000). They have been worked since the 1980s for drilling-grade barite rock, mainly by M-I Drilling Fluids UK Ltd. a subsidiary of the Schlumberger company M-I SWACO. Over 1 million tonnes have been mined at Foss with a similar amount remaining unworked at depth (BGS/ODPM, 2006) due to complex folding which causes difficulties in mining (Swenson et al. 1981). Some 5 km along strike to the east in the Ben Eagach-Duntanlich deposit (hereafter simply 'Duntanlich'), a resource of at least 7.5 million tonnes of barite (M-I SWACO, 2014) occurs in a structurally simple, near-vertical tabular orebody. Only the westernmost extremity of this deposit is exposed at surface near the summit of Ben Eagach (Fig. 1b) where small quarrying operations have extracted barite. In 2021, M-I SWACO closed Foss Mine and commenced production from a new underground mine in the Duntanlich orebody.

2.1. Stratigraphy and stratiform mineralization

The Ben Eagach Schist Formation (Fig. 1b and 2), is a heterogeneous metasedimentary package (Sturt, 1961; Treagus, 2000) mainly comprising graphitic quartz muscovite schists that are typically chloritic and garnetiferous where non-mineralized. In mineralized parts of the formation, garnet is absent and disseminated iron sulfides are ubiquitous (Moles, 1985b). Locally the schists are calcareous with thin beds of graphitic dolostone. There are also beds of fine- and coarse-grained quartzite, the latter similar to the Carn Maig Quartzite that stratigraphically underlies the Ben Eagach Schist Formation. The stratigraphically overlying Ben Lawers Schist Formation (Fig. 1b and 2) comprises calcareous and non-sulfidic pelites, and contains barite and chert mineralization only in its lowermost strata. Both pelite formations contain volumetrically minor amounts (<5 %) of metamorphosed mafic igneous rocks, the protoliths of which were tuffaceous sediment and transgressive sills (Coats et al., 1980, 1981). The presence of mafic volcanic components in the host rocks to the Aberfeldy deposits and overlying strata, together with the 'sedex' mineralization, have been interpreted as evidence of high heat flow and convective circulation of hydrothermal fluids during the early stages of crustal extension (Coats et al., 1981; Russell, 1985; Hall, 1993; Treagus, 2000).

Stratigraphically above the Ben Lawers Schist Formation are a variety of tectonostratigraphic units with different formation names along the Dalradian strike. Lateral thickness and facies variations, combined with increasing grades of metamorphism and tectonic dislocation towards the northeast, make some lateral correlations tenuous. In the Aberfeldy area, the Farragon Volcanic Formation (Fig. 2b) is an interbedded sequence of quartzite, psammite, metabasalt and volcanoclastic 'green beds' (Treagus, 2000) representing the earliest major volcanic episode in the Dalradian. Succeeding this is the uppermost formation in the Argyll Group, the predominantly semipelitic Ben Lui Schist Formation. This is overlain by the Loch Tay Limestone Formation, regarded as a lateral equivalent of the Tayvallich Slate and Limestone formations in SW Scotland (Fig. 2). The Tayvallich Volcanic Formation of the SW Highlands is not present as a discrete formation in central Perthshire, although mafic volcanism is represented by conformable amphibolites of intrusive and volcanoclastic origin within the Loch Tay Limestone Formation (we discuss stratigraphic equivalences later). The geochronology of the Tayvallich Volcanic Formation is well established, with a keratophyre dated at 595 ± 4 Ma (multi-grain U-Pb zircon; Halliday et al., 1989) and a tuff bed dated at 601 ± 4 Ma (U-Pb SHRIMP zircon; Dempster et al., 2002). The volcanic rocks are approximately coeval with the pre-metamorphic granites of Keith-Portsoy and Ben Vuirich (Fig. 1a) (Rogers et al., 1989; Pidgeon and Compston, 1992), and together these constitute a major bimodal magmatic event typical of an extensional rift setting during break-up of the Rodinia supercontinent (Tanner et al., 2006; Fettes et al., 2011; Yonkee et al., 2014).

The material of economic value in the Aberfeldy ore deposits is a granoblastic-textured barite rock, often zebra-banded (Fig. 3a and 3c), that occurs as stratiform beds up to several metres thick within mixed siliciclastic and carbonate metasediments. The barite beds are usually sandwiched top and bottom by siliceous rocks referred to as cherts, although some of these are foliated and comprise mainly barium feldspar (celtsian). In some parts of the deposits, carbonate rocks (calcite, dolomite, ankerite) and sulfide rocks (mainly pyrite with lesser sphalerite and galena) occur within the mineralized beds (Coats et al., 1981; Hall, 1993) (Fig. 3b). The mineralized beds typically have sharp boundaries with the metasediments above and below, and clastic sediments are rarely incorporated into the mineralization (Moles et al., 2015). These features suggest rapid deposition of chemical sediments during hydrothermal exhalative episodes that were vigorous but short-lived and episodic, rather than continuous persistent exhalation or mineralization by post-sedimentation diagenetic replacement (discussed further in section 2.2). Seven exhalative episodes are represented in the Foss deposit (from base to top, M1 to M7: Fig. 4a) although Foss Mine

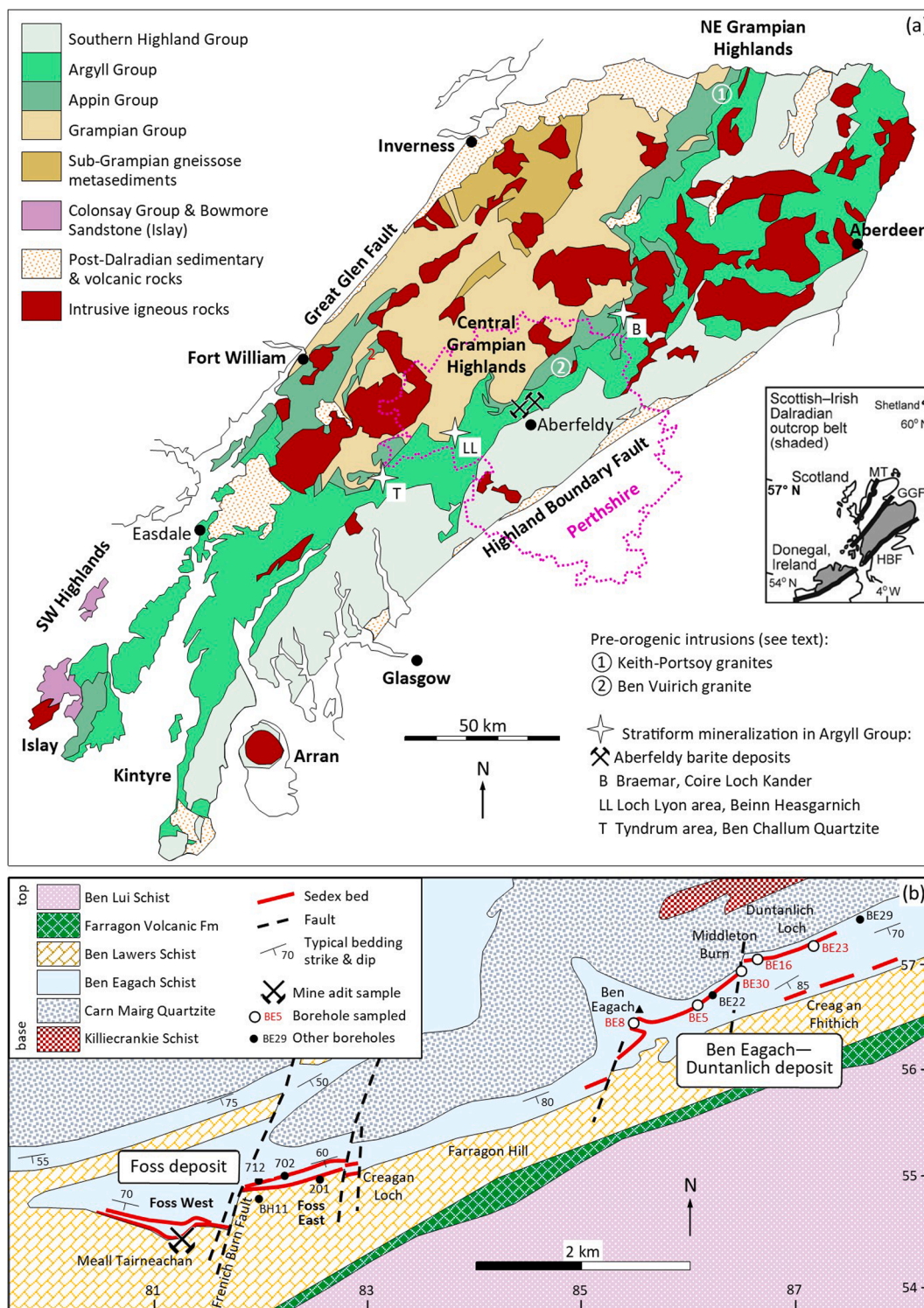


Fig. 1. (a) Simplified geological map of the Grampian Highlands of Scotland, modified from [Thomas et al. \(2004\)](#), showing Dalradian groups and major igneous intrusions. Faults omitted. Numbers identify pre-orogenic granitic intrusions named in the text. Mine symbols show location of the Aberfeldy deposits, letters identify other occurrences of stratiform barium mineralization hosted by Argyll Group metasediments. Dotted line outlines the former county of Perthshire, now the Perth and Kinross District. Inset map from [Prave et al. \(2009a\)](#) shows location of the Dalradian outcrop in Scotland (including the Shetland Islands) and northwest Ireland: MT = Moine Thrust. (b) Bedrock geology in the vicinity of Foss and Ben Eagach–Duntanlich barite deposits adapted from maps by [Coats et al. \(1980\)](#), [Moles \(1985b\)](#) and [Treagus \(2000\)](#) and showing the approximate surface projection of mine adit and drillcore samples analysed in this study. Also shown are locations of Dresser Minerals borehole BE29 (see text) and other boreholes for which stratigraphic profiles are provided in [Fig. 4](#). Marginal two-digit numbers are UK Ordnance Survey kilometre grid eastings and northings.

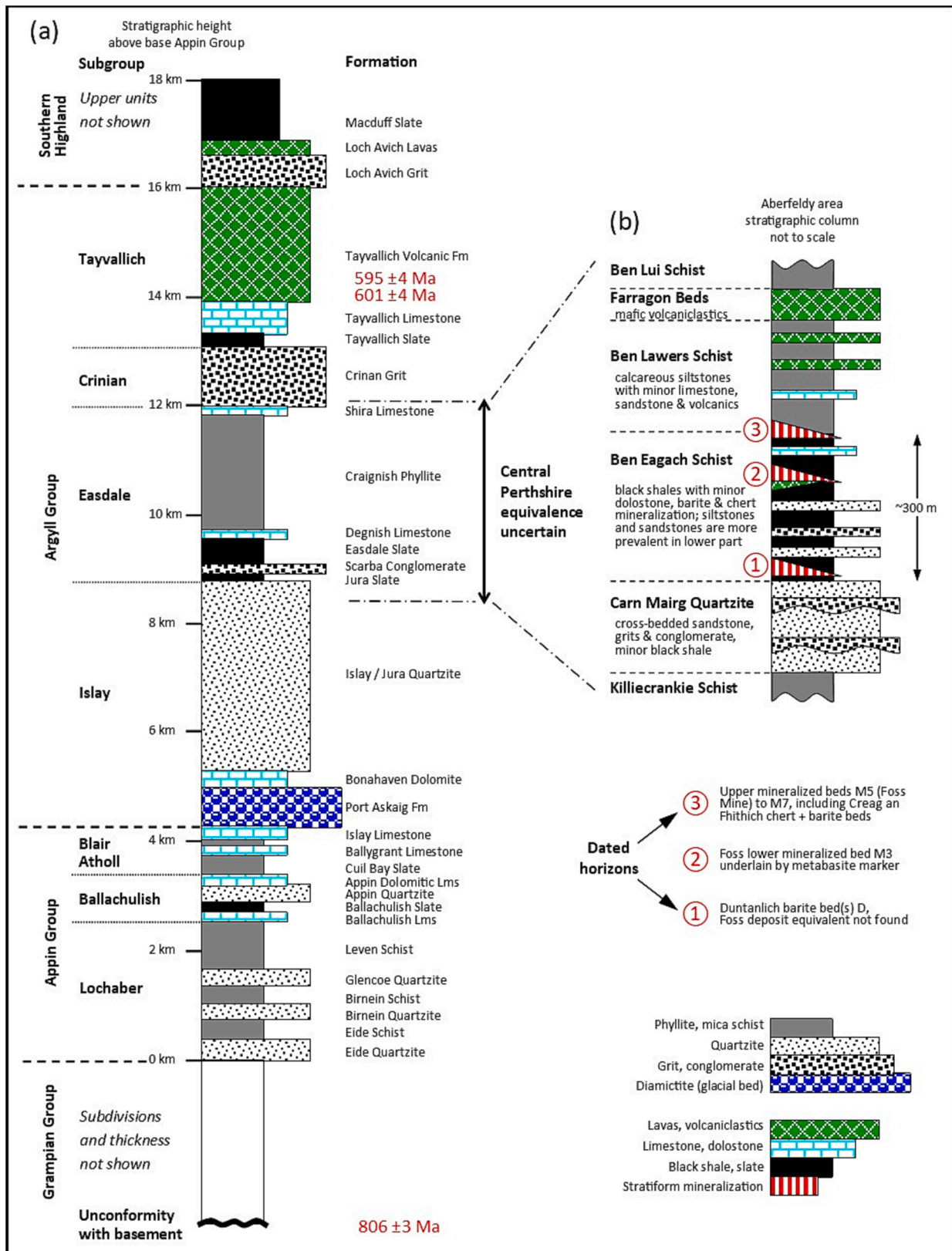


Fig. 2. (a) Formations and sedimentary thickness of the Appin, Argyll and Southern Highland Groups in SW Scotland, from various sources mainly Stephenson et al. (2013). Thicknesses are indicative as they vary laterally (Anderton, 1985). Radiometric dates for the Tayvallich Volcanic Formation from Halliday et al. (1989) and Dempster et al. (2002) and for pegmatites intruding basement underlying the Appin Group from Noble et al. (1996) as interpreted by Strachan et al. (2002). (b) Easdale Subgroup stratigraphy in the vicinity of the Aberfeldy barite deposits (after Ruffell et al. 1998) showing the positions of stratiform mineralization at ① Duntanlich and ②, ③ Foss and of beds dated in this study.

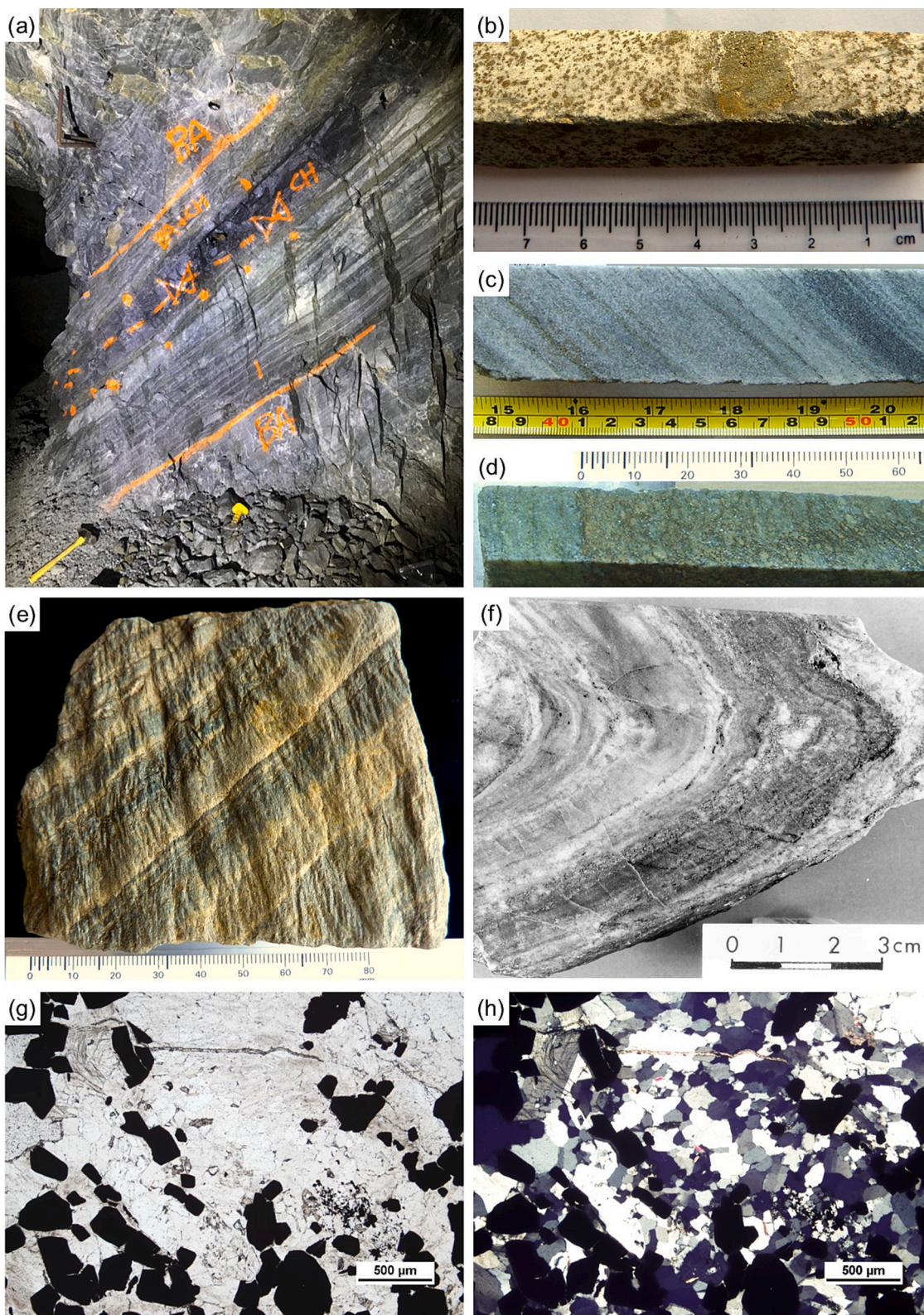


Fig. 3. Textural features of the stratiform mineralization and associated rocks. (a) Foss Mine sampling locality, 545 crosscut (March 2018), showing footwall banded barite-pyrite rock sandwiched within an isoclinal fold of barite rock (labelled 'BAR'). (b) Duntanlich deposit drillcore sample BE5 158.90–159.00 showing granular pyrite in a barite matrix with coarse pyrite crystals at centre. (c) Drillcore from Foss West borehole 80-D424, 216.39–2.16.58 m downhole (top at left) showing banded barite containing disseminated pyrite (left) and magnetite (right). (d) Drillcore from Foss West borehole 80-L429 at 319.60 m downhole showing base of M3 barite bed (left) directly overlying the metabasite marker bed. (e) Ben Eagach Schist outcrop sample from Frenich Burn, Foss East: fine sandstone to laminated siltstone showing graded bedding, overprinted by crenulation cleavage (scale in mm). (f) Cut rock sample from Foss Mine showing small-scale fold within pyritic quartz celsian 'chert'. (g) and (h) Photomicrographs (plane polarised light and crossed-polarised respectively) of a thin section of Foss Mine sample DS3-18 showing disseminated pyrite crystals in a matrix of granoblastic-textured barite. At upper left is celsian with a twin plane cutting across 'snowball' foliation relict from the precursor cymrite. Above the scale bar is a patch of finely-crystalline rutiled quartz.

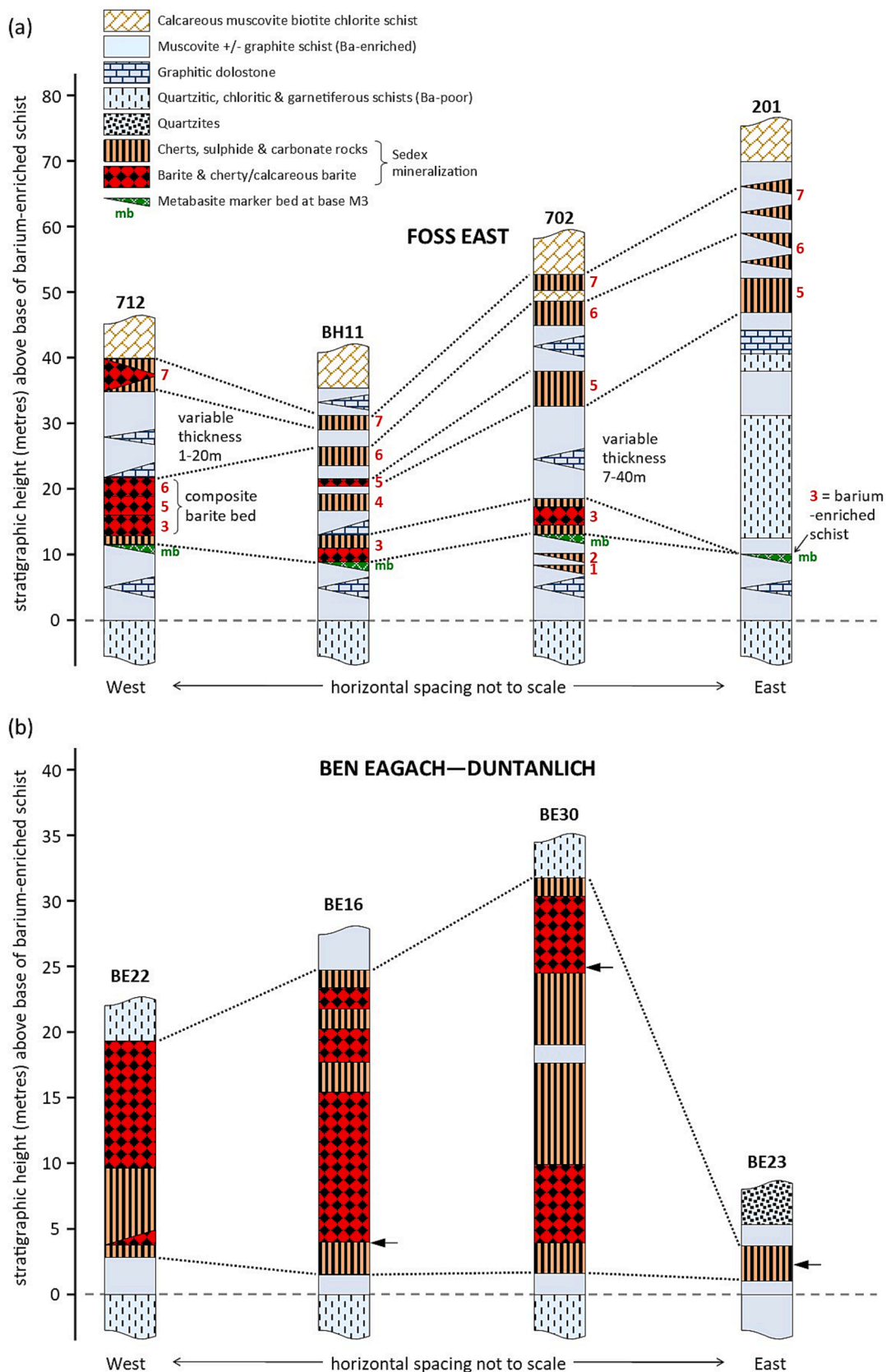


Fig. 4. Representative stratigraphic (interpreted true thickness) sections of (a) the Foss East deposit and (b) the Duntanlich mineralized bed, showing lateral continuity of stratiform beds with lateral facies and thickness changes in mineralization and host sediments. Modified from sections produced by Dresser Minerals geologists (authors in Swenson et al., 1981) with further logging by Moles (1985b). In (a), red numbers alongside profiles indicate the mineralized bed number, M1 to M7. In (b), arrows indicate pyrite sample location. Borehole locations indicated in Fig. 1. (For interpretation of the references to colour in this figure legend, the reader is referred to the web version of this article.)

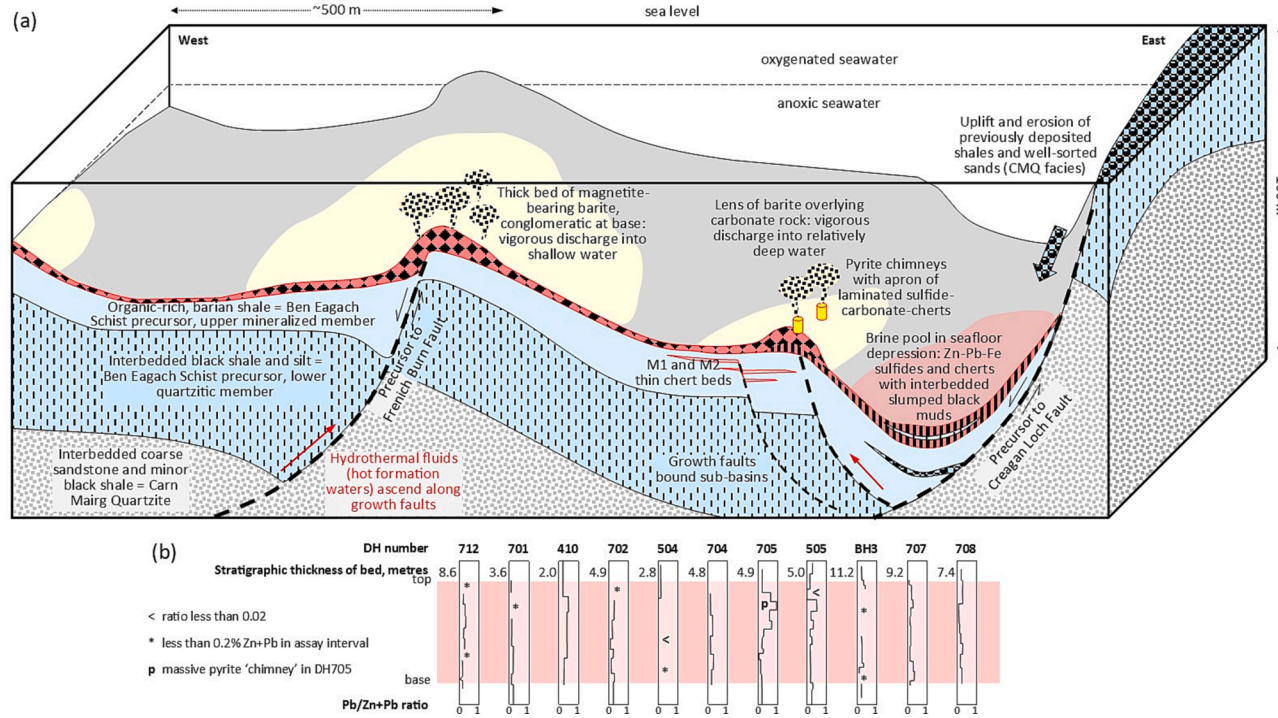


Fig. 5. (a) Conceptual representation of the marine environment during deposition of the first extensive mineralized bed, M3, in the Foss deposit. Variations in the rates and types of sediment input are attributed to localised basal down-warping and uplift associated with syndimentary extensional faulting and rotation of fault blocks. This together with stratification of oxygen levels in the seawater accounts for the synchronous precipitation from the same hydrothermal fluids of barite in shallow water, and of chert, carbonate rock and sulfides in deeper water. Fault uplift and erosion of previously deposited black shales and coarse sands produced debris flows interbedded with the mineralization in a deep-water brine pool at the eastern edge of the deposit. (b) Pb/Zn + Pb ratios in assay intervals of drillcore through the M3 bed in Foss East (data from M-I SWACO and Coats et al., 1981 for BH3; Moles, 1985b). Vertical scale varies: numbers at top left of each plot give stratigraphic thickness in metres of each intersection. Charts are arranged in west-east sequence approximately aligning with the cross-section above. Pb/Zn + Pb ratios approach 1 in upper parts of the DH705 and DH505 drillhole intersections proximal to a postulated hydrothermal vent location.

exploited only the M5 barite bed. The Duntanlich barite 'bed' may similarly comprise the precipitates from several exhalative episodes (Fig. 4b). The hydrothermal exhalations occurred in relatively shallow water as evidenced by localised reworking to form barite conglomerate and stacking of multiple layers of early-cemented barite to form composite beds (Fig. 4a) (Moles et al., 2015).

Stratigraphic correlation within the Foss deposit is facilitated by a single thin, laterally extensive metabasite bed that directly underlies the lower main mineralized horizon ('M3' of Moles, 1985b; Moles et al., 2015) (Fig. 4a). This metabasite marker bed is typically 2–15 cm thick and comprises muscovite-dolomite-quartz-rutile-pyrrhotite schist, or locally biotite- and calcite-rich or K-Na-Ba feldspar-rich schists. Enrichment of K, Ba and CO₂ is ascribed (Moles, 1985b) to alteration associated with weathering and hydrothermal mineralization following deposition of a layer of basaltic ash on the seafloor, coincidental with exhalation of hydrothermal fluids from which the chemical sediments precipitated. A comparable metabasite at the base of Ba-rich stratiform mineralization has not been found at Duntanlich, hindering stratigraphic correlation between the two deposits. A 1 m-thick, barium-enriched chert bed ~ 70 m stratigraphically above the Duntanlich barite horizon in drillhole BE29, beyond the eastern margin of the Duntanlich orebody (Fig. 1b), may be the time-equivalent of the Foss M3 horizon (Fig. 2b). The lateral equivalent of the Duntanlich mineralized bed(s) have not been found in the vicinity of the Foss deposit but potentially occur concealed at depth in Foss East. Fig. 5

Utilising outcrop mapping and approximately 40 drillcore sections of the 2.2 km-long Foss deposit, Swenson et al. (1981) and Moles (1985b) presented evidence for rapid lateral facies and thickness changes, both in the mineralized beds and in the enclosing metasediments. Fig. 5a is a conceptual representation of the dynamic marine environment during deposition of the M3 mineralized bed. A varied seabed topography associated with synsedimentary faulting, together with stratification of oxygen levels in the seawater, accounts for the synchronous precipitation of barite in shallow water, and of chert, carbonate rock and sulfides in deeper water. Barium enrichment in the adjoining schists, hosted cryptically in micas which contain up to 10 wt% Ba (Fortey and Beddoe-Stephens, 1982), extends both stratigraphically and laterally around the mineralization in the Aberfeldy deposits (Willan, 1981). Distal from exhalative sources, mineralized beds taper and are eventually represented just by cryptic barium enrichment at the equivalent horizon (Fig. 4). Across the Grampian Highlands (Fig. 1a) at approximately the same chronostratigraphic level are further occurrences of hydrothermal barium enrichment (Hall, 1993), although these localities do not have barite rock of sufficient purity and volume to be of commercial interest.

Well-preserved 'sedex' / clastic-dominant Zn-Pb-barite deposits are characterized by hydrothermal vents where metalliferous fluids sourced from deep formation waters were exhaled into the contemporaneous sea (e.g. Goodfellow and Lydon, 2007; Leach et al., 2005). Such vents are difficult to discern in the Aberfeldy deposits due to subsequent deformation. Both deposits are bisected by post-metamorphic faults (Frenich Burn Fault and Middleton Burn Fault, Fig. 1b), close to which ore thicknesses and grades are highest. These faults probably re-activated pre-existing faults that acted as channels for the hydrothermal fluids (Fig. 5a). Additionally, a localised vent was intersected by Dresser Minerals borehole DH705 in Foss East. This borehole penetrated a 2 m interval of massive pyrite central within the M3 bed, associated with laminated sulfidic chert-carbonate rock in which Pb/(Zn + Pb) ratios are unusually high (Moles, 1985b). Elevated ratios are found at the same stratigraphic level in adjoining intersections within a strike-length of ~ 100 m (Fig. 5b). These features are not easily explained by a diagenetic replacement model, and support a synsedimentary origin of the mineralization.

2.2. Post-depositional modification, preservation of primary mineralogy

In the mid-Ordovician Grampian Orogeny, some ~ 130 Myr after

deposition of the uppermost Dalradian strata, the beds were tilted and distorted by several phases of folding (Fig. 3f) and faulting, and subjected to medium-grade, amphibolite facies regional metamorphism (Treagus, 2000; Treagus et al., 2013). Timing of the metamorphic maxima varied across the Dalradian outcrop but in Perthshire the peak conditions, associated with porphyroblast growth, lasted about 10 Myr from c. 474 to c. 464 Ma followed by relatively rapid cooling and uplift (Dempster, 1985; Stephenson et al. 2013). In the vicinity of the Foss deposit, metamorphic conditions reached 530 ± 30 °C and 9 ± 1 Kbar (Moles, 1985a). Rock textures and structure have been strongly modified by regional metamorphism and associated ductile deformation, particularly evident in Foss Mine (Swenson et al., 1981). Fig. 6

Notwithstanding metamorphism, the mineralogical components of barite, sulfides, carbonates, iron and titanium oxides, and barium aluminosilicates were considered by previous authors to reflect the original mineralogy of the chemical sediment (Coats et al., 1981; Fortey and Beddoe-Stephens, 1982; Hall, 1993) as this assemblage is typical of 'sedex' barite – Zn-Pb sulfide deposits globally (e.g. Goodfellow and Lydon, 2007; Leach et al. 2005; Leach et al. 2010). However, such assemblages are also typical of shale-hosted stratabound barite deposits formed by diagenetic replacement processes (e.g. Kelley et al., 2004; Fernandes et al., 2017; Magnall et al., 2020; Rajabi et al., 2020). For example, in describing the Teena Zn-Pb deposit (McArthur Basin, Australia), Hayward et al. (2021) show evidence across multiple scales for mid-diagenesis replacement-style Zn-Pb sulfide stratiform mineralization that occurred following sediment compaction at least 400 m below the palaeosurface. Although metamorphism has complicated textural interpretations, there is little evidence for mid-diagenesis formation, such as replacement fronts that cut across bedding, in the Aberfeldy bedded barite-sulfide mineralization. Here, textural evidence for diagenetic dissolution of barite and sulfide replacement is scarce and restricted to volumetrically minor lithologies namely barium-carbonate-bearing sulfide-carbonate-barite rocks and silicified sediments containing sulfate crystal pseudomorphs (Fortey and Beddoe-Stephens, 1982). The barium carbonate minerals barytocalcite, norsethite and (rarely) witherite occur as tiny (<200 µm) inclusions within larger crystals of non-carbonate minerals, predominantly pyrite and occasionally quartz, barite, or sphalerite (Moles, 1985b), but are not found within the main rock mass. In some samples of bedded mineralization, millimetre-diameter pyrite crystals are packed with dozens of tiny inclusions (Fig. 6c). We interpret these features as indicating barium carbonates were abundant during early diagenesis, implying very low sulfate ion concentrations and high carbonate ion concentrations in porewater, characteristics consistent with microbial sulfate reduction and methanogenesis (Moles and Boyce, 2019). During later diagenesis, the non-encapsulated barium carbonates were replaced by matrix barite + non-barian carbonate (i.e. calcite or dolomite). In order for early diagenetic species to be encapsulated in pyrite crystals, the pyrite must have formed during early diagenesis and subsequently coarsened, as shown schematically in Fig. 6e.

Diverse sphalerite compositions are commonly retained within the stratiform mineralization and are interpreted as 'primary' (Moles, 1983). Sphalerite inclusions in pyrite (and occasionally within other minerals) show a wide range of iron contents, indicated qualitatively by variable colours in transmitted light (Fig. 6a), whereas matrix sphalerite shows a narrow compositional range due to post-depositional recrystallization and homogenization. Similarly, within the mineralized beds, sulfur isotope compositions of barite and sulfides appear to have been largely unaffected by metamorphism (cf. Muller et al., 2017) as they are heterogeneous over distances of a few millimetres, as illustrated by laser ablation analyses of individual disseminated pyrite crystals (Fig. 6d).

In contrast to the compositionally heterogeneous pyrite found in some carbonate-hosted stratabound ores (such as Lisheen, Ireland: Hnatyshin et al., 2020), pyrite in the Foss and Duntanlich deposits is homogeneous within individual crystals in terms of trace elements, a feature consistent with recrystallization during high pressure regional

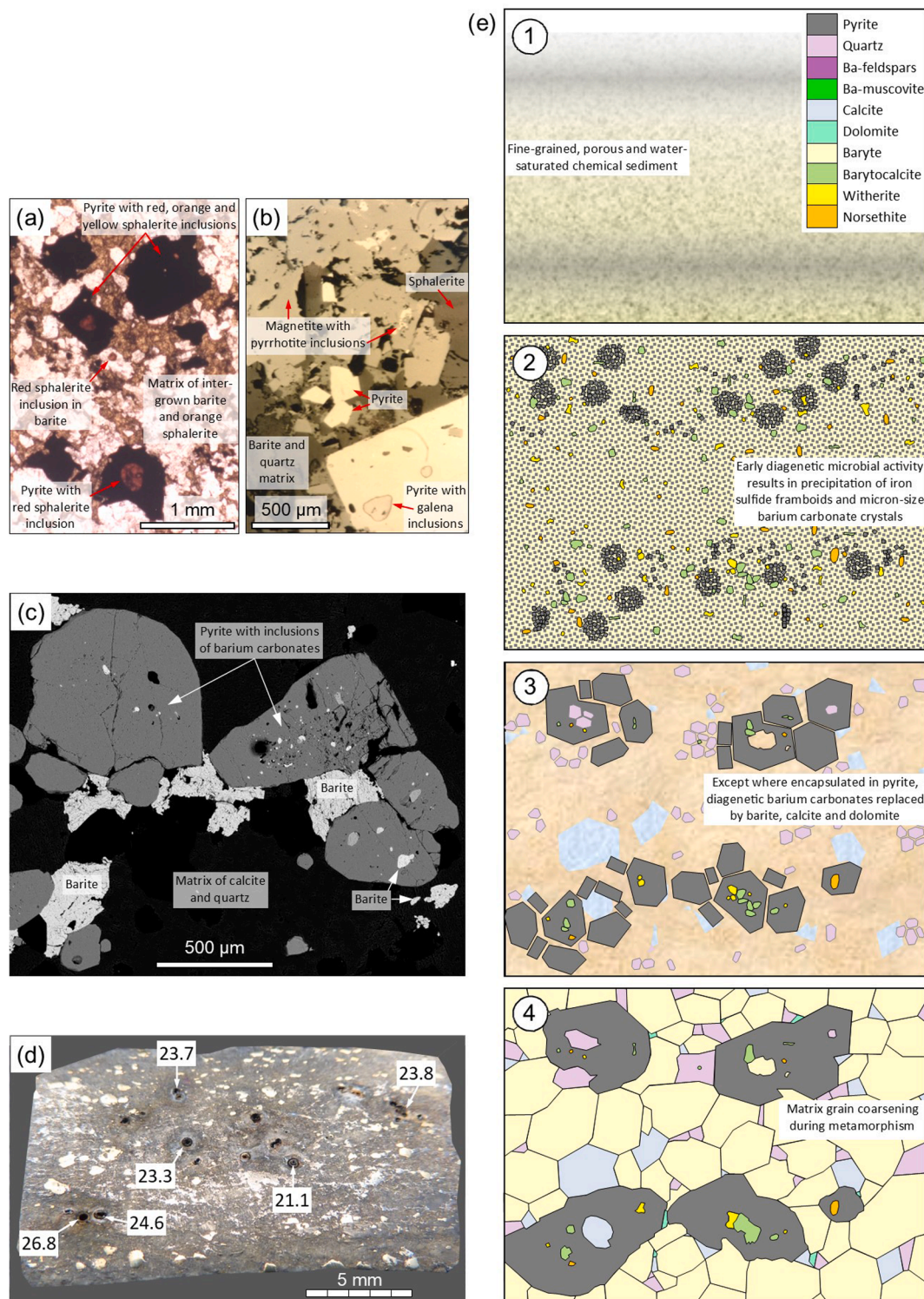


Fig. 6. Microtextural features of pyrite and associated minerals in the stratiform mineralization. (a) Transmitted light photomicrograph of sulfidic barite rock containing pyrite (black) and both iron-rich and iron-poor sphalerite (red and orange respectively). Volumetrically subordinate red sphalerite is mainly encapsulated by pyrite: one small red grain enclosed by barite is visible near centre. Foss East sample 705–20. (b) Reflected light photomicrograph showing subhedral magnetite and euhedral pyrite, both adjoining sphalerite in quartz barite rock. Small round inclusions of galena occur in the large pyrite, irregular inclusions of pyrrhotite in the magnetite. Foss East sample 702–7. (c) Back-scattered electron image of pyrite crystals in a matrix of barite, calcite and quartz. Pyrite aggregates contain abundant small barium carbonate inclusions. Foss East sample 702-4B. (d) Polished block of a laminated chert with pyrite crystals containing barium carbonate inclusions, showing pyrite crystals analysed by laser ablation and the obtained $\delta^{34}\text{S}$ values in per mil (‰). Foss East sample 505–15. (e) Interpretative reconstructions of textural and mineralogical evolution during (1) deposition, (2) early diagenesis, (3) late diagenesis and lithification, and (4) regional metamorphism of typical chemical sediment in the Aberfeldy deposits. Sketches represent vertical sections of sediment / rock approximately 3 mm tall and 4 mm wide. (For interpretation of the references to colour in this figure legend, the reader is referred to the web version of this article.)

Table 1
Sample details and results of Re-Os analysis of pyrite from the Foss and Ben Eagach–Duntanlich barite deposits.

Deposit	Sample no.	Position (X, Y: Ordnance Survey National Grid; Z: height in metres above average sea level datum)	Total Re (ppb)	±	Total Os (ppt)	±	¹⁸⁷ Re (ppb)	±	¹⁹² Os (ppt)	±	¹⁸⁷ Re/ ¹⁸⁸ Os	±	¹⁸⁷ Os/ ¹⁸⁸ Os	±	rho [^]	% Re blank	% ¹⁸⁷ Os blank	% ¹⁸⁸ Os blank	Os-i*	Os-i*	±
Foss	DS1-18	X = 281239.978 Y = 754455.880 Z = 541.711	19.00	0.07	331.6	1.1	11.94	0.04	80.1	0.3	471.8	2.6	5.56	0.03	0.535	0.07	0.00	0.1	@ 604 Ma	@ 606 Ma	0.04
	DS1B-18	ditto	19.10	0.07	320.7	1.1	12.00	0.04	76.4	0.3	497.1	2.7	5.74	0.04	0.549	0.03	0.01	0.1	0.72	0.70	0.04
	DS2-18	ditto	17.86	0.06	404.0	1.5	11.22	0.04	110.7	0.6	320.9	2.0	4.01	0.03	0.593	0.07	0.00	0.1	0.77	0.75	0.04
	DS2B-18	ditto	36.38	0.13	434.9	1.9	22.87	0.08	77.9	0.3	929.7	5.1	10.14	0.06	0.552	0.01	0.00	0.1	0.74	0.71	0.08
	DS6-18	ditto	9.84	0.03	210.6	0.6	6.18	0.02	56.1	0.2	348.8	1.9	4.34	0.03	0.554	0.03	0.01	0.1	0.81	0.80	0.03
	DS13-18	ditto	9.00	0.03	750.2	1.5	5.66	0.02	264.9	1.1	67.6	0.4	1.42	0.01	0.544	0.08	0.01	0.1	0.74	0.74	0.01
	DS14-18	ditto	10.57	0.04	362.2	0.9	6.64	0.02	112.6	0.5	186.6	1.0	2.64	0.02	0.538	0.03	0.01	0.1	0.75	0.75	0.02
Duntanlich [#]	BE5-159	X = 286108.476 Y = 756649.069 Z = 428.038	7.44	0.03	854.2	2.0	4.68	0.02	309.4	1.6	47.8	0.3	1.20	0.01	0.587	0.08	0.01	0.03	@ 607 Ma	@ 606 Ma	0.01
	BE8-454	X = 285461.621 Y = 756525.280 Z = 265.352	1.28	0.01	22.0	0.4	0.80	0.00	5.3	0.1	479.3	10.8	5.62	0.17	0.721	0.45	0.07	1.88	0.75	0.76	0.20
	BE16-136.4	X = 286655.915 Y = 757062.223 Z = 344.371	18.17	0.12	597.5	2.9	11.42	0.07	184.8	1.6	195.6	2.1	2.70	0.03	0.571	0.03	0.00	0.06	0.71	0.71	0.04
	BE23-115.9	X = 287158.848 Y = 757245.902 Z = 377.687	5.15	0.02	110.1	0.7	3.24	0.01	29.6	0.3	346.6	3.3	4.25	0.05	0.661	0.11	0.02	0.34	0.72	0.73	0.06
	BE30-512.8	X = 286500.086 Y = 757056.429 Z = 125.391	11.28	0.04	323.4	0.7	7.09	0.03	96.4	0.4	232.6	1.2	3.08	0.02	0.507	0.05	0.01	0.11	0.71	0.72	0.02

[#] Duntanlich sample number incorporates borehole code (locations on Fig. 1b) followed by downhole depth in metres

* initial ¹⁸⁷Os/¹⁸⁸Os calculated using the ¹⁸⁷Re decay constant (plus uncertainty) of Smoliar et al. (1996)

^ rho - error correlation (Ludwig, 1980)

all uncertainties 2 s

metamorphism (e.g. Walters et al., 2019). Electron microprobe analyses of Aberfeldy pyrites (Moles, 1985b) show they contain trace Cu (<0.07 %), Ni (<0.12 %) and Co (0.02–0.21 %). The typically low Co and Ni contents and high Co/Ni ratios suggest a sedimentary affiliation (e.g. Gregory et al., 2015). Mukherjee and Large (2017) observed that pyrite-hosted Ni, Co and Mo decrease in proximity to Australian Proterozoic ‘sedex’ deposits, in comparison to pyrite distal from exhalative activity. Previous petrographic and sulfur isotope studies of pyrite in the Dalradian Easdale Subgroup showed that early diagenetic pyrite framboids, preserved as inclusion-rich cores, are overgrown by later, inclusion-poor, euhedral pyrite (Hall et al. 1988; Hall et al. 1994). These conclusions are supported by LA-ICP-MS mapping of element distributions within pyrite crystals (Parnell et al., 2017) which show arsenic enrichment in cores typical of early diagenetic pyrite, and Pb-enriched euhedral overgrowths formed during metamorphism.

Within some Aberfeldy barite rock, magnetite forms rounded grains up to 2 mm (modal concentration < 5 %), either disseminated or concentrated into laminae and occasionally monomineralic bands ~ 1 cm thick. Sulfides commonly adjoin or are encapsulated as inclusions in magnetite crystals (Fig. 6b), again suggesting syngenetic or early diagenetic crystallization. Electron microprobe analyses of Foss deposit magnetite indicate trace element (Al, Ti, Cr, Mn) concentrations generally near or below detection limits (Moles, 1985b). Magnetite is found only in relatively thick barite beds associated with vent-proximal shallow water locations (Fig. 5) where vigorous mixing of the hydrothermal fluids with oxygenated seawater resulted in an oxygen fugacity sufficiently high enough for iron oxides to precipitate instead of iron sulfides (e.g. Nadoll et al., 2014). Incorporation of atmospheric oxygen into the barite is evidenced by mass-independently fractionated oxygen isotope (O-MIF) signals with $\Delta^{17}\text{O}$ values as low as -0.249 (mean: -0.179 ‰; $n = 7$) (Moles et al., 2020). The paucity of sulfides in the Ben Lawers Schist, and in barite beds M6 and M7 in the uppermost part of the Ben Eagach Schist (Fig. 2b and 4a), is consistent with increased oxygenation of the sea bed at this time, possibly corresponding to one of the episodic ocean oxygenation events that occurred in the Ediacaran (Yuan et al., 2022).

3. Sampling and methods

3.1. Samples for re-Os analysis

Table 1

Five pyrite-bearing samples from the barite bed worked in Foss Mine were collected in March 2018 from a fresh exposure (Fig. 3a) at an elevation of 542 m above Ordnance Datum beneath Meall Tairneachan (‘mine adit sample’, Fig. 1b). Two samples (DS1-18 and DS2-18) were several kilograms in weight and these were split into two non-adjacent sub-samples with one sub-sample from each labelled as ‘B’, generating a total of 7 samples for analysis (Table 1). The samples are from a pyritic unit ~ 20–30 cm in thickness within an isoclinally folded bed of barite rock corresponding to the M5 exhalative event (Fig. 3a and 4), and comprise predominantly barite and pyrite, with minor quartz and celsian, and trace dolomite, phlogopite and rutile (Fig. 3g and 3 h). The modal abundance of pyrite is up to 30 %. The barium feldspar celsian has textural features that are typical of the platy mineral cymrite which has been pseudomorphed by celsian after fabric development when the peak metamorphic temperature was attained (Fortey and Beddoe-Stephens, 1982; Moles, 1985a). Granoblastic textures and an absence of internal strain in crystals also indicate that annealing followed deformation.

Five pyrite-rich samples of drillcore from the Duntanlich deposit were obtained from Dresser Minerals 1980s drillcore stored in M-I SWACO’s premises in Aberfeldy (representative intervals are archived in the National Geological Repository, BGS Keyworth Core Store). Sampling intentionally targeted widely-spaced intersections of the mineralized bed across a strike length of 2 km (Fig. 1b). Sample depths range

from ~ 125 to ~ 425 m above sea level (Ordnance Datum); sample names indicate borehole number and downhole depth in metres (Table 1). The samples comprise pyrite-barite rock and pyrite-rich quartz-calcite-celsian rocks (Fig. 3b-d) with up to 35 % pyrite by volume. They are from both the footwall (e.g. BE23-115.9) and hanging-wall (e.g. BE16-136.4 and BE30-512.8) of the main barite bed (Fig. 4b).

To prepare pyrite mineral separates, the rock samples were crushed without metal contact and sieved to obtain a 70 to 200 mesh fraction, and this fraction was then hand-picked under a light microscope to obtain a visually pure mineral separate. For each sample ~ 0.5 g of pyrite was separated. Lastly the samples were placed in 0.2 N HCl and left at room temperature for 24 h prior to analysis to remove any mineral impurities (e.g., dolomite, oxides). This process has been shown to remove impurities without adversely affecting the re-Os systematics of pyrite (Hnatyshin et al., 2020; Paradis et al., 2020). The 0.2 N HCl was then decanted, and the sample thoroughly rinsed with milli-Q water and then with ethanol prior to drying.

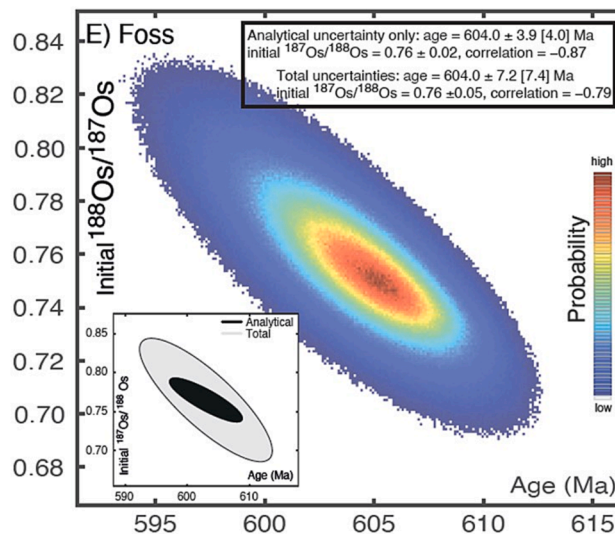
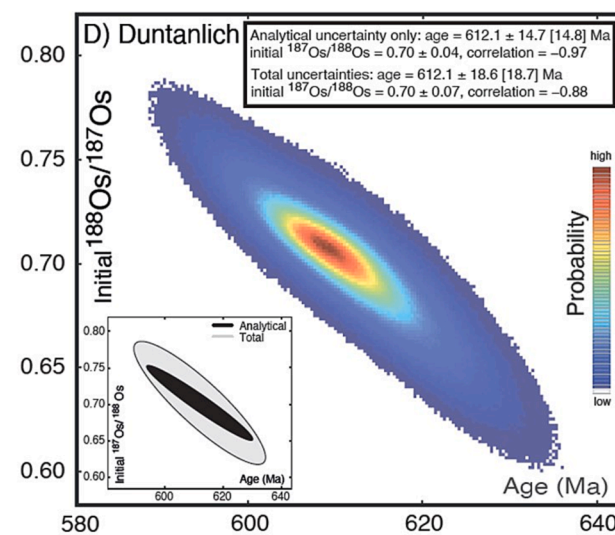
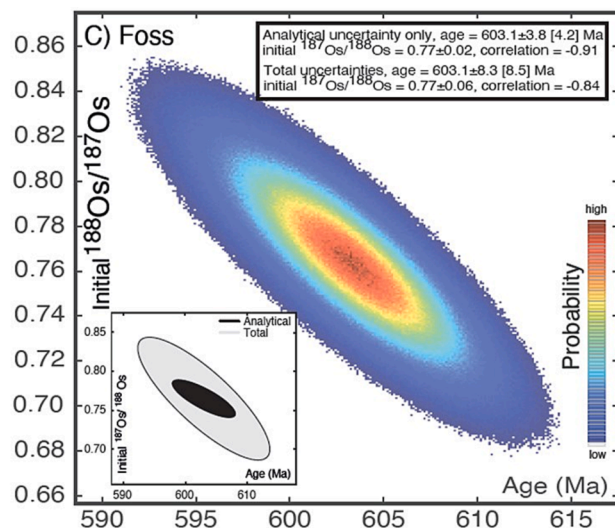
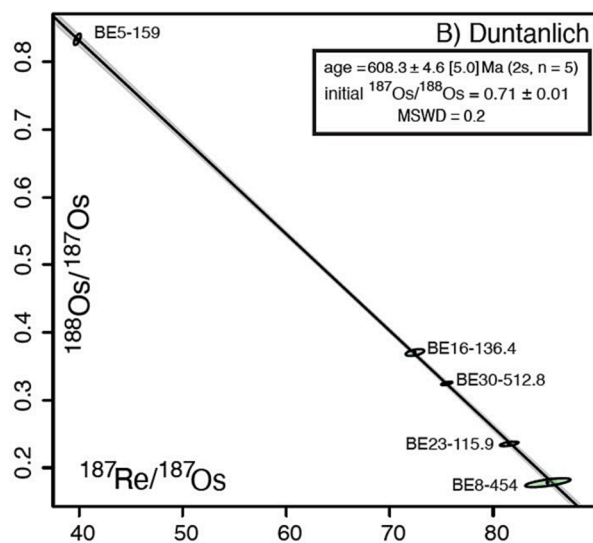
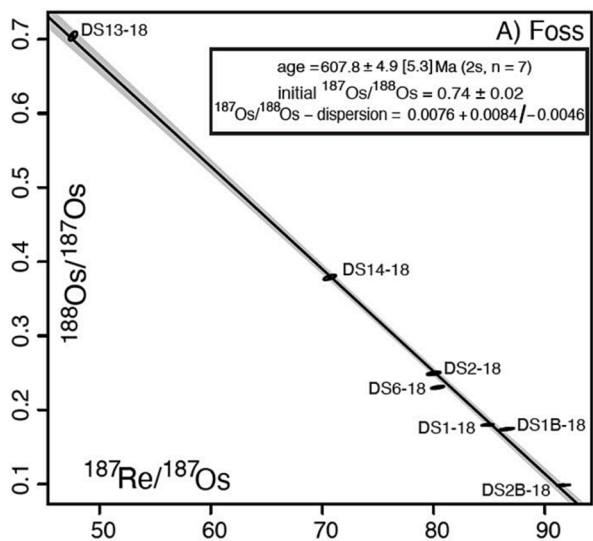
Molybdenite tends to be enriched in Re and ^{187}Os and can be problematic for re-Os studies if present as impurities within pyrite separates (e.g. Hnatyshin et al., 2020). However, in detailed microscopic and SEM studies of the Aberfeldy deposits (Moles, 1985b and unpublished work on Duntanlich), molybdenite has not been reported. Care was taken to ensure that the analysed samples contained no magnetite, as this can also be problematic for pyrite Re-Os studies.

3.2. Analytical protocols

Rhenium-osmium analyses were carried out at the Durham Geochemistry, in the Source Rock and Sulfide Geochemistry and Geochronology and Arthur Holmes Laboratories, following published protocols (Selby et al., 2009; Li et al., 2018a). Approximately 0.4 g aliquots of each sample were weighed and placed in to a carius tube together with a known amount of a mixed tracer solution ($^{185}\text{Re}+^{190}\text{Os}$) and 9 mL of inverse aqua regia (3 mL 11 N HCl and 6 mL 15 N HNO_3). The carius tube was then sealed and placed in an oven at 220 °C for 48 hrs to dissolve the pyrite and equilibrate the sample and tracer Re and Os. The Os was extracted and purified from the acid solution by CHCl_3 solvent extraction and $\text{CrO}_3\text{-H}_2\text{SO}_4\text{-HBr}$ microdistillation. The Re fraction was obtained by NaOH-Acetone solvent extraction and HCl- HNO_3 anion chromatography (Cumming et al., 2013; Selby and Creaser, 2003). The isotope composition of the Re and Os fractions were determined on a Thermo Scientific TRITON mass spectrometer via static Faraday collection and ion-counting using a secondary electron multiplier in peak hopping mode, respectively. Total procedural blanks were 3.1 ± 1.6 pg for Re and 0.15 ± 0.13 pg for Os, with a $^{187}\text{Os}/^{188}\text{Os}$ of 0.19 ± 0.04 ($n = 4$). Two in-house Re (ReSTD) and Os (DROs) solutions were used to monitor the long-term reproducibility of the mass spectrometer isotope measurements, which during this study (2019) yield an average $^{187}\text{Re}/^{185}\text{Re}$ and $^{187}\text{Os}/^{188}\text{Os}$ of 0.59834 ± 0.0004 and 0.16088 ± 0.0066 (1 S.D., $n = 6$). The re-Os isotopic data including 2 s calculated uncertainties for $^{187}\text{Re}/^{188}\text{Os}$ and $^{187}\text{Os}/^{188}\text{Os}$ and the associated error correlation function (ρ) were regressed using both IsoplotR’s inverse isochron approach (Li and Vermeesch, 2021) and the Monte Carlo sampling method (Li et al., 2018b) for error propagation to yield a Re-Os age using the ^{187}Re decay constant of $1.666e^{-11} \pm 5.165^{-14}\text{a}^{-1}$ (Ludwig, 1980; 2011; Smoliar et al., 1996).

4. Re-Os results

Pyrite from both Foss ($n = 7$) and Duntanlich ($n = 5$) possess similar contents of Re (9.0 – 36.4 [average and 1SD – 17.4 ± 9] vs 1.3 – 18.2 [8.7 ± 6.4] ppb), total Os (211 – 750 [402 ± 169] vs 22 – 854 [381 ± 345] ppt) and ^{192}Os (56 – 265 [111 ± 71] vs 5 – 309 [125 ± 124] ppt), respectively (Table 1). Pyrite $^{187}\text{Re}/^{188}\text{Os}$ and $^{187}\text{Os}/^{188}\text{Os}$ ratios also show considerable overlap (Foss $^{187}\text{Re}/^{188}\text{Os} = 68 - 930$ [403 ± 277], $^{187}\text{Os}/^{188}\text{Os} = 1.42 - 10.14$ [4.84 ± 2.80] and Duntanlich $^{187}\text{Re}/^{188}\text{Os}$



(caption on next page)

Fig. 7. (a) Re-Os data from seven samples yield an inverse isochron of 607.8 ± 5.3 Ma (2σ , including decay constant uncertainty) and an initial $^{187}\text{Os}/^{188}\text{Os}$ (Os-i) value of 0.74 ± 0.02 using an inverse isochron approach (Li and Vermeesch, 2021) for the Foss deposit. (b) Re-Os data from five samples from the Duntanlich deposit yield an inverse isochron of 608.3 ± 5.0 Ma (2σ , including decay constant uncertainty) and a Os-i value of 0.71 ± 0.01 . (c) A Monte Carlo simulation (Li et al., 2018b) for the Re-Os data of the Foss deposit yielded results within uncertainty to those from an inverse isochron approach ($603.1 \pm 4.2/8.5$ Ma; uncertainties are presented as analytical only/model uncertainty including decay constant), and indicates that analytical uncertainty is 42 % of uncertainties for the final age (inset plot). The determined Os-i is 0.77 ± 0.06 . (d) Distribution of age and Os-i estimates based on the Monte Carlo approach using the Re-Os for the Duntanlich deposit ($612.1 \pm 14.8/18.7$ Ma, Os-i = 0.70 ± 0.07). Inset shows total uncertainty at the 2σ level and the contribution to the total from analytical and model uncertainty. Analytical uncertainty accounts for 81 % of the total. (e) A Monte Carlo simulation for the Re-Os data of the Foss deposit without samples DS1B-18 and DS6-18 yielding the best estimate for the Re-Os age (604.0 ± 7.2 [7.4] Ma [including total model uncertainties with and without the decay constant uncertainty], and Os-i = 0.76 ± 0.05) of the mineralization. See text for discussion.

= 48 – 479 [260 ± 162], $^{187}\text{Os}/^{188}\text{Os}$ = 1.20 – 5.62 [3.37 ± 1.67] (Table 1).

Using IsoplotR’s inverse isochron approach (Vermeesch, 2018; Li and Vermeesch, 2021), the Re-Os pyrite data from Foss yield a Model 3 date of 607.8 ± 4.9 [5.3; including ^{187}Re decay constant uncertainty]

Ma (2 s, initial $^{187}\text{Os}/^{188}\text{Os}$ [Os-i] = 0.74 ± 0.02 [dispersion = 0.0076 + 0.0084 / – 0.0046], Mean Squared Weighted Deviates [MSWD] = 7.6 [determined from Model 1], n = 7, Fig. 7a). The Re-Os data of pyrite from Duntanlich yield a Model 1 age of 608.3 ± 4.6 [5.0] Ma (2 s, Os-i = 0.71 ± 0.01 , MSWD = 0.2, n = 5, Fig. 7b).

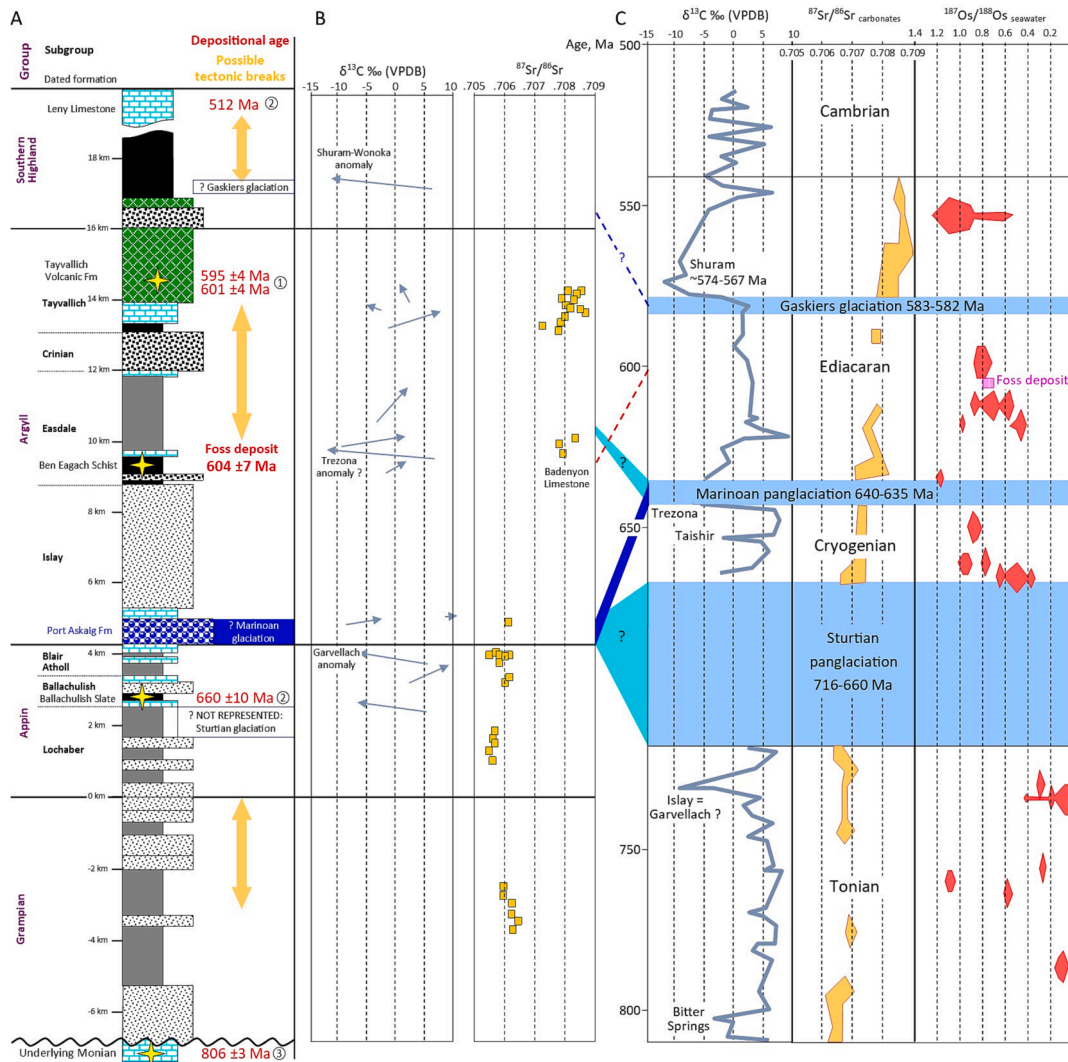


Fig. 8. Geochronological and chemostratigraphical constraints on the depositional age of formations in the Dalradian Supergroup. (a) Stratigraphy as in Fig. 2a: formations and sedimentary thickness are based on SW Scotland. Stars identify dated formations: ① Halliday et al. (1989) and Dempster et al. (2002), ② Rooney et al. (2011), ③ Noble et al. (1996), with addition of the Ben Eagach Schist-hosted stratiform pyrite Re-Os age reported here for the Foss deposit. Double-headed arrows indicate potential locations of tectonic breaks proposed by Dempster et al. (2002). (b) Carbon and strontium isotope chemostratigraphic profiles for Dalradian limestones, derived from Prave et al. (2009a,b) and Fairchild et al. (2018). $\delta^{13}\text{C}$ trends indicated by arrows with the names of pronounced negative excursions suggested by these authors. (c) Global compilation of Neoproterozoic $\delta^{13}\text{C}$, strontium isotope, and osmium isotope trends respectively from compilations by Cox et al. (2016), Fairchild et al. (2018) and Manoel et al. (2021) and references therein. Refer to Fig. 6 of Manoel et al. (2021) for data sources for $^{187}\text{Os}/^{188}\text{Os}_{\text{seawater}}$ derived from organic-rich sedimentary rock analyses. Magenta box labelled ‘Foss deposit’ shows range and mean value of Aberfeldy pyrite Os-i at 606 Ma (Table 1). Connecting (b) and (c) are alternative possible correlations of the Port Askaig Formation with either the Sturtian (light blue) or Marinoan (dark blue) panglaciations (see text). (For interpretation of the references to colour in this figure legend, the reader is referred to the web version of this article.)

Given the importance of obtaining robust timing constraints utilising the isochron approach, concerns of underestimating uncertainties using Isoplot, and to quantify contributions of uncertainty from analytical and model age assumptions (Li et al., 2018a,b), here the Monte Carlo simulation approach is applied to obtain Re-Os pyrite ages and Os-i for Foss and Duntanlich. Including both analytical and model uncertainty (total uncertainty), Re-Os ages for Foss are 603.1 ± 8.3 Ma [8.5 including ^{187}Re decay constant uncertainty] (Os-i = 0.77 ± 0.06 , analytical uncertainty contribution is 42 %, Fig. 7c), and for Duntanlich, 612.1 ± 18.6 [18.7] Ma (2 s, Os-i = 0.70 ± 0.07 , analytical uncertainty contribution is 81 %, Fig. 7d).

For Foss, the adoption of a Model 3 regression and a MSWD > 1 in IsoplotR suggest that the re-Os data of the Foss sample set are over dispersed with respect to the analytical uncertainties, and clearly indicate the presence of scatter related to geological factors (e.g., different formation times, variation in Os-i, disturbance to re-Os systematics). This interpretation is supported by the Monte Carlo simulation, which suggests that analytical uncertainties only account for 42 % of the total uncertainties. Since samples DS1B-18 and DS6-18 show the greatest deviation from the linear regression line (Fig. 7a), excluding these samples yields a Model 3 inverse isochron Re-Os date of 608.0 ± 2.7 [3.3] Ma (Os-i = 0.73 ± 0.01 [dispersion = $0.000071 + 0.00063/-0.000071$], MSWD = 3 [determined from Model 1]) by IsoplotR and 604.0 ± 7.2 [7.4] Ma (Os-i = 0.76 ± 0.05 , analytical uncertainty contribution is 49 %) by the Monte Carlo simulation. The cause of the deviation from the linear regression line of samples DS1B-18 and DS6-18 is not known, but could be a combination of open system behaviour of Re-Os isotopes, non-identical Os-i or pyrite not formed simultaneously. Here we consider the Monte Carlo outcome of the Re-Os data for five of the seven samples from Foss to provide the best estimate for the Re-Os age (604.0 ± 7.2 [7.4] Ma, and Os-i = 0.76 ± 0.05) (Fig. 7e) as the methodology makes no prior assumption for the cause of variability in the data set and propagates uncertainties from both analytical and model sources. Our data corresponds with the explanation of Hnatyshin et al. (2020, section 5) which discusses the acceptance of Model 3 linear regressions.

For Duntanlich samples, the Monte Carlo simulation clearly demonstrates the underestimation of uncertainties in Isoplot's Model 1 approach which only accounts for analytical uncertainties, hence we consider the Monte Carlo results as the best age estimate (612.1 ± 18.6 [18.7] Ma, Os-i = 0.70 ± 0.07) (Fig. 7d).

5. Discussion

5.1. Significance of pyrite Re-Os ages and Os-i for ore genesis and source of Re and Os

Our analyses also show that Re-Os ages for pyrite from the Foss and Duntanlich deposits are identical within uncertainty. This is not unexpected considering the short stratigraphic interval that hosts the mineralized beds: in the study area the Ben Eagach Schist Formation comprises up to ~ 300 m of mainly clastic metasedimentary strata (Fig. 2b and 4) which was likely to have been deposited within a couple of million years (Moles et al., 2015). Pyrite from laterally widely-spaced samples in the Duntanlich deposit yielded a Re-Os age and Os-i that are similar to closely-spaced samples from the Foss deposit, indicating that both deposits formed semi-contemporaneously and also from fluids derived from the same source. Sub-seafloor replacement processes, such as advocated for Phanerozoic clastic-dominant stratabound Zn-Pb ± Ba deposits (e.g. Magnall et al., 2020) involve the introduction of hot (~300 °C) hydrothermal fluids into the shallow subsurface (<1 km depth) within a million years or so following primary deposition of the host sediments. Pyrite Re-Os dating with uncertainties of a few million years would not be able to distinguish mineralization formed by such replacement processes from syn-sedimentary or early diagenetic formation. For example, using Re-Os dating, Reynolds et al. (2021)

demonstrate that diagenetic mineralization occurred very soon after deposition of the host sedimentary rocks in the Anarraaq clastic-dominant Zn-Pb-Ag and barite deposit (Red Dog district, Alaska). However, post-depositional hydrothermal replacive processes would likely produce a greater scatter in pyrite Os-i ratios and Re-Os ages, such as observed in base metal sulfide deposits where mineralization formed or was modified over protracted periods (e.g. Hnatyshin et al., 2020). In the Aberfeldy stratiform mineralization, a protracted period of pyrite formation is not favoured by textural evidence including encapsulation of early diagenetic barium carbonates and millimetre-scale diversity in sulfur isotope values (Fig. 6) as discussed above. If a proportion of the pyrite precipitated some time after the synsedimentary mineralization, the bulk pyrite Re-Os ages reported here would be younger than the host rock age, perhaps by a few million years.

The close similarity of the Aberfeldy pyrite Re-Os age to radiogenic age estimates for the depositional age of strata a few kilometres stratigraphically higher, discussed below, strongly indicates that the pyrite Re-Os system survived the regional metamorphism of the mid-Ordovician Grampian Orogeny. This is consistent with both experimental and field observations for the Re-Os systematics of pyrite from other mineral systems that experienced post-ore amphibolitic-eclogitic metamorphic conditions (e.g. Brenan et al., 2000; van Acken et al., 2014; Vernon et al., 2014). Conversely, the Re-Os systematics of graphite appear to be substantially altered in high-temperature metamorphism. Toma et al. (2022) report a very low Re content of 0.6 ppb in a sample of graphite from Foss Mine (their sample UNXX-SUK) which X-ray diffraction studies indicate crystallized at 601 °C. This contrasts with Re contents of hundreds or thousands of ppb that are typical of graphite in metasedimentary rocks subjected to lower temperature metamorphism, implying that Aberfeldy graphite is unsuitable for Re-Os dating of sedimentation.

Fig. 8

Adopting the Monte Carlo method as the best estimate for the Re-Os age, the age estimation of 604.0 ± 7.2 Ma for the Foss deposit (Fig. 7) provides a valuable new geochronological marker within the Dalradian Supergroup (Fig. 8a). Wider correlation of this age for the deposition of the Ben Eagach Schist / Easdale Subgroup is afforded by other occurrences of Ba-rich stratiform mineralization at the same stratigraphic level: low-grade barite-Zn-Pb sulfide mineralization occurs in the Ben Eagach Schist Formation along strike from Aberfeldy in the Loch Lyon area (Beinn Heasgarnich) and at Coire Loch Kander ~ 10 km SE of Braemar (Fig. 1a) (Gallagher et al., 1989). Stratiform barium mineralization is also associated with the Easdale Subgroup Lakes Marble Formation (age not yet quantified) in Connemara, western Ireland (Reynolds et al., 1990; Harris et al., 1994). In the Tyndrum area of central-western Grampian Highlands (Fig. 1a), quartzite-hosted stratabound Zn-Cu-Pb mineralization (Fortey and Smith, 1986; Hill et al., 2015) occurs in the stratigraphically higher Ben Challum Quartzite, considered by some to be a lateral equivalent of the volcanoclastic Farragon Beds in Perthshire (Stephenson et al., 2013) (Fig. 2).

The initial $^{187}\text{Os}/^{188}\text{Os}$ (Os-i) in pyrite from the Foss (0.76 ± 0.05) and Duntanlich (0.70 ± 0.07) deposits are similar, overlapping within uncertainty (Table 1). These values are typical of mid-Ediacaran seawater osmium isotope ratios (Fig. 8c). The early-mid Ediacaran differentiation and radiation of macroscopic eukaryotes was associated with highly fluctuating oceanic redox conditions and Os- $_{\text{seawater}}$ values (Yang et al., 2022). We infer a single, homogenous source of osmium and by inference metals in fluids from which pyrite, or a precursor iron sulfide, precipitated. The moderately radiogenic initial $^{187}\text{Os}/^{188}\text{Os}$ values of Aberfeldy iron sulfides are consistent with both a seawater origin or a crustally derived osmium component (and by inference Re and other elements) in the mineralizing fluids. Magmatic activity in the area during and after sedimentation was minimal (as noted above) and mafic magmatism is unlikely to be the source of Os incorporated in pyrite. A hydrothermal / basinal fluid derivation of Re and Os (and other elements) would be consistent with other components of the Aberfeldy

stratiform mineralization, specifically strontium. Small inclusions of strontium-bearing barite and carbonate crystals, including barium carbonates, encapsulated within pyrite (Fig. 6c) demonstrate that Sr was incorporated at the time of deposition and/or early diagenesis (Moles, 1985b; Moles and Boyce, 2019). Six Sr isotope analyses of 4 barite samples from the Foss Open Pits (barite quarries located east of the underground mine in Foss West), reported by Hall et al. (1991), yielded initial $^{87}\text{Sr}/^{86}\text{Sr}$ of 0.71340–0.71505 with a median of 0.714. This initial $^{87}\text{Sr}/^{86}\text{Sr}$ matches the initial $^{87}\text{Sr}/^{86}\text{Sr}$ of the Appin Group Dalradian sequence (Fig. 8) below the Ben Eagach Schist Formation which led Hall et al. (1991) to propose that the Sr incorporated in barite was derived dominantly from the basinal hydrothermal solution that had interacted with the Dalradian sequence and not the contemporaneous seawater which had a significantly less radiogenic composition (as shown in Fig. 8, $^{87}\text{Sr}/^{86}\text{Sr}$ of Neoproterozoic seawater ranged from 0.707 – 0.709; Veizer, 1989).

5.2. Evidence for uninterrupted deposition of the upper Argyll Group succession

Calculations of sedimentation rates based on stratigraphic thickness may help to resolve whether upper Argyll Group stratigraphy in the central Grampian Highlands of Scotland represents a period of continuous sedimentation, or could incorporate a hiatus possibly associated with orogenic uplift (Fig. 8a). First we need to review the stratigraphic equivalence with dated formations in the SW Highlands. The Tayvallich Volcanic Formation (595 ± 4 Ma: Halliday et al., 1989; 601 ± 4 Ma: Dempster et al., 2002), comprising a thick sequence of largely mafic rocks, lies at the top of the Argyll Group in SW Scotland (Fig. 8a). As stated above, volcanic rocks are scarce at this stratigraphic position in the central Highlands. Stratigraphic correlation of the Tayvallich lavas with the Loch Tay Limestone in the central Highlands is a long-held assumption, largely based on lateral continuity of calcareous formations (Craignish Phyllite, Ben Lawers Schist) and equivalence of the Crinan Grit with the Ben Lui Schist (Crinan Subgroup: Fig. 8a) (Stephenson et al., 1995; Stephenson et al., 2013; Treagus, 2000; Treagus et al., 2013). In the central Highlands, the main episode of mafic volcanism in the Argyll Group is represented by the Farragon Beds within the upper Easdale Subgroup (Fig. 2b). This implies that volcanism initiated considerably earlier here than in the SW Highlands. An alternative interpretation is that the main episode of mafic volcanism was synchronous across the Scottish Dalradian such that the Tayvallich Volcanic Formation is stratigraphically equivalent to the Farragon Beds. Such an equivalence would better accommodate the geochronological overlap in depositional ages of the Ben Eagach Schist (our results for Foss pyrite: 604 ± 7 Ma) and the Tayvallich Formation (601 ± 4 Ma based on Dempster et al., 2002). Considering more widely the timing of Rodinian rifting, an apatite U-Pb age of 613 ± 12 Ma for a mafic lava in the Ediacaran Browns Hole Formation of Idaho (Provow et al., 2021) in conjunction with 601 ± 27 Ma for a gabbroic sill in central Idaho (Brennan et al., 2020), suggests that rift-related (possibly mantle plume) magmatism may have occurred synchronously across the western Laurentian margin.

Returning to the Scottish Dalradian, if we assume that the long-established correlations are correct, the ~ 601 Ma Tayvallich Volcanics are between 3000 m and 5000 m stratigraphically above the ~ 604 Ma Ben Eagach Schist Formation (our dating) and its lateral equivalent, the Easdale Slate Formation (Fig. 2a and 8). Considering the stratigraphic thicknesses known in the SW Highlands, where orogenic deformation is less intense than in Perthshire, this would indicate a net average sedimentation rate of 0.75 to 1.25 mm per year (0.75–1.25 m/kyr), accommodation space permitting. By comparison, Provow et al. (2021) calculated a Brigham Group sedimentation rate of ~ 0.64 m/kyr

from the end of the Marinoan glaciation at ~ 635 Ma to eruption of mafic lava at ~ 613 Ma in the Browns Hole Formation. These rates are compatible with continuous sedimentation through this period, given that episodic deposition occurs on a sub-millennial timescale (Kemp et al., 2018) and that clastic sedimentary successions typically represent only a small portion of elapsed time (Sadler, 1981; Miall, 2014). Our inference of uninterrupted and relatively rapid sedimentation accords with that of Thomas et al. (2004) who suggested, based on global correlations using Sr isotope ratios of Dalradian limestones (cf. Shields et al., 2021), that the middle and upper parts of the Argyll Group were deposited in a short time period (Fig. 8b).

However, several researchers have postulated unconformities within the Argyll Group sequence in NW Ireland and SW Scotland. Pitcher and Berger (1972) argued for an unconformity at the base of the Easdale Subgroup in County Donegal, NW Ireland. Subsequently, Hutton and Alsop (2004) reported evidence from this region that the lower strata of the Dalradian Supergroup may have been deposited and undergone deformation (pre-600 Ma) prior to deposition of the upper strata (i.e. post-600 Ma). This deduction was based principally on (i) a complete excision of quartzites of the Islay Subgroup, (ii) an unconformity below the Stralinchy Conglomerate in County Donegal, and (iii) compressional deformation fabrics that are developed within clasts in this conglomerate and the underlying formations (Alsop et al., 2000) but are absent from stratigraphically higher formations. Dempster et al. (2002) postulated a depositional break within the Argyll Group (Fig. 8A) based on evidence of polymetamorphism in the lower parts of the Dalradian Supergroup that is absent in the upper strata, and contact metamorphic mineral assemblages that are incompatible with sedimentary thicknesses in the aureole of the pre-orogenic Ben Vuirich Granite (Fig. 1a). Stratigraphic and structural evidence for the existence of a base-Easdale Subgroup tectonic unconformity was contested by Tanner (2005) who argued that field data from the SW Highlands of Scotland do not support an orogenic unconformity in the Easdale Subgroup, but instead point to sporadic large-scale debris flows that formed basin margin slump–slide deposits. In response, Alsop and Hutton (2005) suggest that the conglomerates and breccias in the two sequences of NW Ireland and SW Scotland are sedimentologically and stratigraphically unrelated, and reiterate their original conclusion that an unconformity and tectonic break are present at the base of the Easdale Subgroup in Donegal.

The occurrence of ikaite pseudomorphs in the Kerrara Slate of SW Scotland (considered to be stratigraphically equivalent to the Easdale Slates and Ben Eagach Schist formations) was presented by Dempster and Jess (2015) as evidence for ultra-low temperature metamorphism and deep penetration of extremely low temperatures below an unconformity in the overlying strata, associated with a prolonged ‘snowball Earth’ episode. On this basis, they conclude that an orogenic unconformity must be present between the formations of the Easdale Slate and the Tayvallich Volcanics. Although the textural evidence implies syn-metamorphic ikaite growth, it could be argued that the ikaite may be pre-metamorphic and the pseudomorphs survived subsequent Ordovician Grampian orogeny metamorphism.

Our Re-Os dating of the lower to middle-Easdale Subgroup in central Perthshire does not directly resolve this controversy which will require dating of Argyll Group formations underlying the Ben Eagach Schist / Easdale Slate equivalents in SW Scotland and NW Ireland. However, we argue against regional metamorphism of the underlying formations, since metamorphism would greatly reduce their permeability and potential to supply barium-, strontium- and base-metal-enriched hydrothermal fluids (heated formation waters) to form exhalative mineralization. Such mineralization occurs widely in the Easdale Subgroup not only in Scotland but also, as noted above, in western Ireland. Indeed, the existence of large-volume hydrothermal mineral deposits at this stratigraphic level indirectly speak to the permeability of the

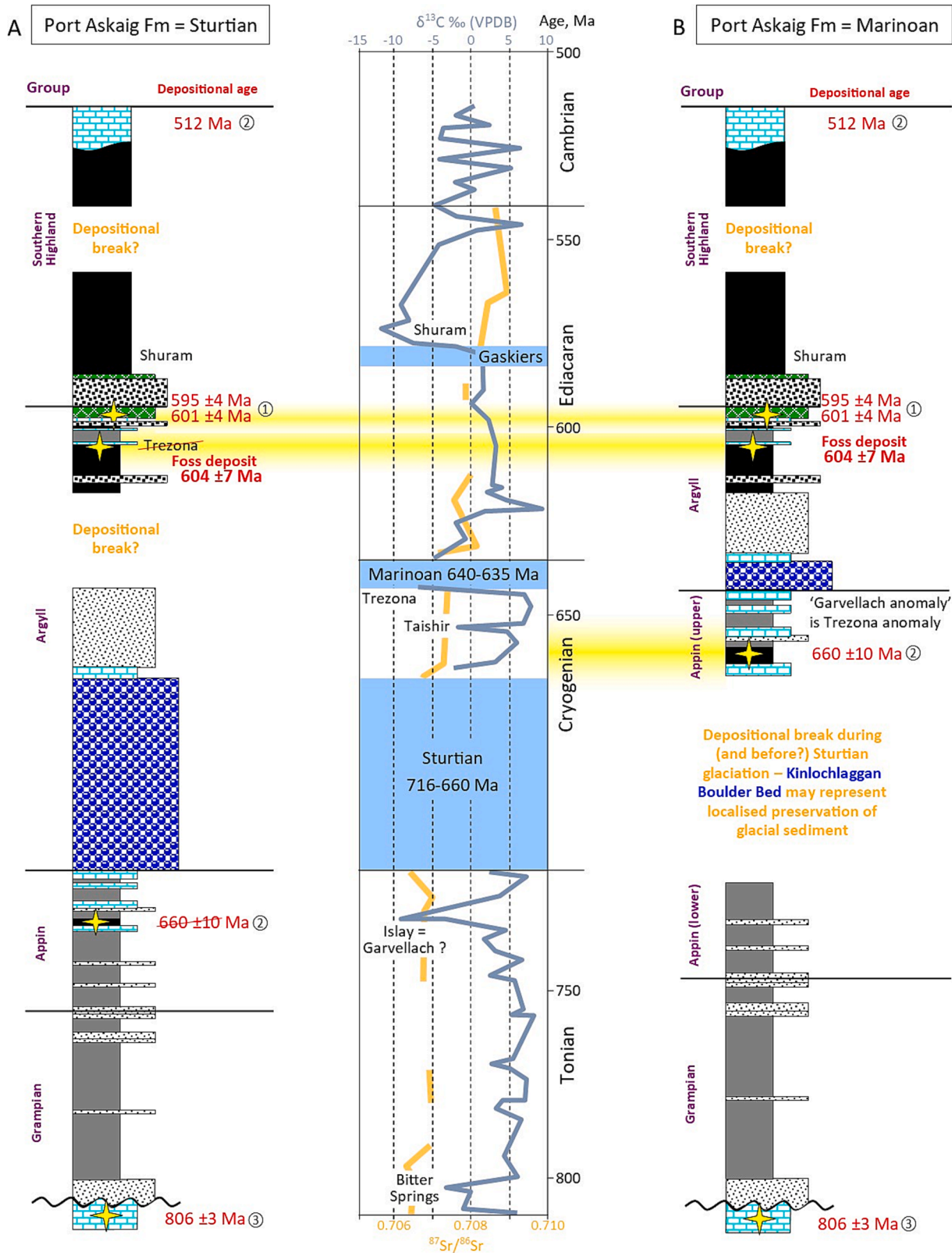


Fig. 9. Centre: Late Neoproterozoic to lower Cambrian timeline with Sr isotope and $\delta^{13}\text{C}$ curves as per Fig. 8c, labelled with glacial periods indicated by blue shading and globally recognised $\delta^{13}\text{C}$ excursions (Shields-Zhou et al., 2016; Halverson et al., 2020; Shields et al., 2021). A: Dalradian stratigraphy fitted to the timeline using Argyll Group geochronological markers (yellow horizontal bands indicate error ranges; for sources refer to Fig. 8a caption) and assuming a Sturtian correlation of the Port Askaig Formation. This necessitates a depositional break in the Marinoan-equivalent period and negates Appin Group correlation of the ~ 660 Ma date of Rooney et al. (2011). B: Dalradian stratigraphy fitted to the timeline using a Marinoan correlation of the Port Askaig Formation, which validates Rooney et al.'s upper Appin Group date and necessitates an underlying depositional break perhaps corresponding to the prolonged Sturtian glaciation. Positions of postulated depositional breaks are hypothetical and require confirmation from field evidence and further geochronological research. (For interpretation of the references to colour in this figure legend, the reader is referred to the web version of this article.)

underlying strata at the time of mineralization, regardless of whether this was synsedimentary or syndiagenetic.

5.3. Implications of Re-Os dating for global correlation of Dalradian glaciogenic formations

Several researchers have attempted to correlate the Dalradian sequence to the western Laurentian margin and global Neoproterozoic record using chemostratigraphy and occurrences of glaciogenic formations (e.g. Shields-Zhou et al., 2016). In this regard, an important stratigraphic marker is the Port Askaig Formation ('Port Askaig Tillite' or 'Boulder Bed' in older literature) which defines the base of the Argyll Group (Fig. 2a and 8a). This diamictite has been variously ascribed to the Marinoan glaciation ~ 635 Ma (e.g. Evans and Tanner, 1996; Brasier and Shields, 2000; Stephenson et al., 2013), or to the Sturtian glaciation 717–662 Ma (e.g. Dempster et al., 2002; McCay et al., 2006; Prave et al., 2009; Prave and Fallick, 2011), or to either of these (Rooney et al., 2014). Rooney et al. (2011) reported a depositional Re-Os age of 659.6 ± 9.6 Ma for the Ballachulish Slate Formation which underlies the Port Askaig Formation (Fig. 2a), and consequently they argued against the Sturtian correlation of this glaciogenic sequence. Subsequently, Rooney et al. (2014) back-tracked on this assertion and presented three possible scenarios, one of which is that the presumed 'Ballachulish Slate' near Loch Leven may actually correlate with formations in the Argyll Group, similar to the suggestion by Evans and Tanner (1996) that the Kinlochlaggan Boulder Bed found near Loch Leven is correlative with the Port Askaig Tillite rather than occurring with the Appin Group stratigraphy as previously inferred (Treagus, 1969; 1981).

Fairchild et al. (2018) and others have continued to correlate the Port Askaig Formation with the Sturtian glaciation, based largely on evidence from strontium isotope studies by Sawaki et al. (2010), expanding on work by Thomas et al. (2004), which show that limestones underlying the Port Askaig have exceptionally low $^{87}\text{Sr}/^{86}\text{Sr}$ values (<0.7065 , Fig. 8c). These are characteristic globally of the seawater Sr isotope composition preceding the Sturtian glaciation when intense weathering of flood basalts was associated with initial break-up of the Rodinia supercontinent (Cox et al., 2016; Halverson et al., 2017; Shields and Veizer, 2002; Shields et al., 2021). Given this correlation of the Port Askaig Fm with the Sturtian glaciation, several authors have attributed the apparent absence of Marinoan glaciogenic deposits in the Scottish Dalradian stratigraphy to deep-water re-sedimentation that purportedly 'destroyed' any record of this glacial episode (McCay et al., 2006; Prave et al., 2009a; Fairchild et al., 2018). However, in many places worldwide the Marinoan glaciation is represented by a very thin cap carbonate (sometimes less than a few tens-of-cm thick) and the deep-water glacial deposits themselves consist of rare, dispersed dropstones lacking diamictic beds (e.g. Hoffmann et al., 2004).

Fig. 9

Prave et al. (2009a) identified four significant negative $\delta^{13}\text{C}$ excursions in Dalradian limestones and correlated these to excursions recognised in Neoproterozoic sections globally (Fig. 8b, c). The youngest negative $\delta^{13}\text{C}$ excursion recorded in the Dalradian is in the Grlsta Limestone of Shetland, central within the Southern Highland Group (Fig. 8b). Prave et al. (2009a, b) correlate this with the global late Ediacaran Shuram-Wonoka anomaly and comment that this is consistent with the age of stratigraphically underlying Tayvallich Volcanic Formation. Recently, using samples from two paleo-continents, Rooney et al. (2020) constrained the Shuram-Wonoka anomaly to between 574.0 ± 4.7 and 567.3 ± 3.0 Ma, significantly younger than the Tayvallich Volcanic Formation. The Grlsta Limestone is therefore likely to have been deposited in this time period.

In NW Ireland, the Easdale Subgroup dropstone-bearing Stralinchy-Reelan Formation has been tentatively correlated with the Marinoan glaciation by McCay et al. (2006) who noted the lithological similarity of the overlying Cranford Limestone to cap carbonates. Prave et al. (2009a) report negative $\delta^{13}\text{C}$ excursions below and above this glaciogenic unit,

and conclude that these excursions correlate with the Trezona cap carbonate excursions associated with the Marinoan glaciation (e.g. Rose et al. 2012). The Stralinchy-Reelan Formation lies stratigraphically above the Degnish-Ardrihaig-Craignish formations, of which the lateral equivalent in Scotland is probably the upper part of the Ben Lawers Schist Formation (Fig. 2b). Our ~ 604 Ma date for the immediately underlying Ben Eagach Schist Formation (Easdale Slate equivalent) indicates that either this stratigraphic correlation is incorrect (as discussed above with regard to mafic volcanism), or that the Easdale Subgroup negative $\delta^{13}\text{C}$ excursions (Fig. 8b) are significantly younger than the Marinoan glaciation and do not represent the Trezona anomaly.

The negative $\delta^{13}\text{C}$ excursion beneath the presumed Sturtian Port Askaig Formation was named the 'Islay anomaly' by Prave et al. (2009a) and subsequently renamed the 'Garvellach anomaly' by Fairchild et al. (2018) (Fig. 8b). We suggest an alternative correlation that this excursion represents the pre-Marinoan global Trezona excursion, whereas the Ballachulish Subgroup negative $\delta^{13}\text{C}$ anomaly represents the pre- or post-Sturtian global excursion, albeit with no representation of Sturtian glacial deposits in the Dalradian succession (Fig. 8c, 9b). This argument is conceptually equivalent to that mentioned above to explain the apparent absence of Marinoan glacial sediments.

According to Prave et al. (2009a), the Ballachulish Limestone and equivalents at the base of the Appin Group (Fig. 2a) record the oldest $\delta^{13}\text{C}$ excursion in Dalradian rocks that can be correlated to a global event, namely the ~ 800 Ma Bitter Springs anomaly. However, this was contested by Rooney et al. (2011) who, using Re-Os geochronology, proposed a much younger depositional age of ~ 660 Ma for the Ballachulish Slate (though they subsequently back-tracked as mentioned above). As we discuss below, the negative $\delta^{13}\text{C}$ excursion recorded in the Ballachulish Limestone, immediately below the Ballachulish Slate (Fig. 2a), may equate with the global excursion preceding the Sturtian glaciation.

Chew et al. (2009) presumed a Sturtian age for a Port Askaig-equivalent metadiamictite in the NE Grampian Highlands, the Auchnahyle Formation, and on this basis concluded that an immediately underlying basaltic pillow lava represents the oldest volcanic activity recorded in the Dalradian succession. They suggested this implied an early, local phase of proto-Iapetan rifting within the Rodinian supercontinent. The case for this anomalous early rifting episode vanishes if this diamictite and the correlative Port Askaig Formation are actually Marinoan in age.

5.4. Stratigraphic position of possible breaks in Dalradian sedimentation

Dempster et al. (2002) argued cogently for at least one, if not two or three, major depositional breaks within the ~ 350 Myr Dalradian sequence. They suggested looking for tectonic duplication and thickening that could mark an orogenic episode that would have produced greenschist-facies metamorphism (the earliest phase of the polymetamorphism) reaching a maximum grade in the Appin and Argyll Group rocks of Central Perthshire. Their preferred model is a late Precambrian (pre-590 Ma) orogenic break within the Southern Highland Group that spans the period ~ 600–470 Ma. However, in Fig. 6 of Dempster et al. (2002) a break near the top of the preceding Argyll Group is suggested (Fig. 8a). Our ~ 604 Ma date for Foss deposit pyrite, and by extension, Easdale Subgroup sedimentation, appears to preclude a break within the middle to upper parts of the Argyll Group, as we have shown that sedimentation was apparently continuous from the Easdale Subgroup through the Crinian and Tayvallich Subgroups. This would be the case regardless of uncertainty in the details of stratigraphic correlation and thicknesses that we discussed above.

The question arises as to where in the stratigraphy a break could be accommodated lower within the Argyll Group. In the vicinity of the Aberfeldy barite deposits, there is no evidence of an unconformity between the Carn Mairg Quartzite and Ben Eagach Schist although the boundary is typically abrupt rather than transitional (Fig. 4). The Carn

Mairg Quartzite is characterised by quartz grains that are often coloured blue due to the Tyndall scattering effect caused by microscopic inclusions. As mentioned above, similar quartzites occur locally as thin (<1 m) beds within the stratigraphically overlying Ben Eagach Schist Formation (Moles, 1985b) where they are often cemented by Zn-Pb sulfides lacking barium enrichment (i.e. stratabound mineralization not of hydrothermal origin). The coarse sands in these 'Carn Mairg Quartzite'-type beds were probably eroded from the underlying strata and redeposited in debris flows during rift-related disturbance (Fig. 5). Such reworking would be very unlikely if the underlying strata had been metamorphosed prior to deposition of the Ben Eagach Schist Formation.

Therefore, a depositional break, if one or more actually exist, in the Argyll Group must precede deposition of the Easdale Subgroup. In Fig. 8a we have placed this hypothetically at the top of the Islay Subgroup – though there is no evidence for such a break, and we proceed to reject this interpretation. Rooney et al.'s (2011) Re-Os date for the Ballachulish Slate does not fit with the scenario, represented in Fig. 8a, that the Port Askaig to Islay Subgroup sequence is Cryogenian. Nor does the identification (by Fairchild et al., 2018 and previous authors) of the Trezona anomaly positioned stratigraphically above the Ben Eagach Schist, which we have shown is ~ 30 Myr younger than the Marinoan glaciation.

Our preferred scenario is shown in Fig. 8b in which we correlate the Port Askaig Formation to the Marinoan and show no breaks in deposition within the Argyll Group and upper Appin Group. This fits well with a ~ 660 Ma date for the Ballachulish Slate Formation (Rooney et al. 2011) (if we accept that this date does indeed represent Appin Group sedimentation, cf. Rooney et al., 2014), provided that a substantial depositional break is accommodated stratigraphically below the Ballachulish Limestone within the Appin Group or underlying Grampian Group. We suggest this break would correspond to the prolonged Sturtian glaciation, as shown in Fig. 8b. In this scenario, the Garvellach negative $\delta^{13}\text{C}$ excursion of Fairchild et al. (2018), equivalent to the Islay anomaly of Prave et al. (2009a), may actually be the pre-Marinoan Trezona anomaly. The un-named negative carbon isotope excursion below this (Fig. 7b) may perhaps be the pre-Sturtian global excursion. Our suggestion would reinstate as Sturtian in age the Kinlochlaggan Boulder Bed (Evans and Tanner, 1996). This may be a localised occurrence of Sturtian glacial sediments not preserved elsewhere at this stratigraphic level (Fig. 9b).

Dempster et al. (2002) remark that prolonged breaks in sedimentation are likely to have occurred during the two Cryogenian global 'snowball Earth' episodes and suggest that significant gaps in Dalradian history may be hidden within these depositional breaks. We argue that a prolonged break within the Appin Group occurred during the Sturtian glaciation, and this depositional hiatus was not associated with an orogenic event. As argued previously by Dalziel and Soper (2001), a purely extensional tectonic regime in the Neoproterozoic for the Scottish promontory of Laurentia accords with the stratigraphy of the Greenland and North American Cordilleran / Appalachian sectors where no tectonic breaks are recorded between the Grenvillian and Grampian-equivalent orogenies. In his reconstruction of the Rodinia supercontinent, Dalziel (1991) showed that Laurentia straddled the equator at ~ 750 Ma, and a subsequent clockwise rotation moved the location now occupied by Scotland to > 30°S by ~ 650 Ma (Torsvik et al., 1995). Evans and Tanner (1996) inferred this equatorial location as an explanation for the absence of Sturtian glaciogenic deposits in Baltica and NE Laurentia including the Dalradian block.

5.5. Implications of a probable Marinoan age for the Port Askaig Formation

The global correlation of glaciogenic formations in the Dalradian Supergroup remain controversial. Since early in the 21st Century, the majority of geologists have accepted the laterally persistent Port Askaig Formation and its meta-diamictite correlatives as representing the

Sturtian glacial episode and, as mentioned above, global compilations incorporate Dalradian-derived data on carbonate $\delta^{13}\text{C}$ and $^{87}\text{Sr}/^{86}\text{Sr}$ based on this correlation. Indeed, the sub-Sturtian negative $\delta^{13}\text{C}$ excursion is known globally as the 'Islay anomaly', although Fairchild et al. (2018) suggested renaming this the Garvellach anomaly since at this locality in SW Scotland the anomaly is within limestone conformably underlying the Port Askaig Formation (see also Shields-Zhou et al., 2016).

The new geochronological constraint, combined with previous Re-Os dating of the upper Appin Group (Rooney et al., 2011) if this stratigraphic association is valid, favour a Marinoan (~640–635 Ma) correlation for the Port Askaig Formation. Previously many authors have constructed geological scenarios based on a Sturtian age (~716–660 Ma) of this diamictite and the associated low $^{87}\text{Sr}/^{86}\text{Sr}$ ratios and negative $\delta^{13}\text{C}$ excursion in the underlying limestone, named the Islay or Garvellach anomaly (Shields-Zhou et al., 2016; Halverson et al., 2020). We acknowledge that the low strontium isotope values of < 0.7065 reported by Sawaki et al. (2010) in the Islay Limestone are not characteristic of the Marinoan glaciation globally, and this requires further investigation. Shields et al. (2021) demonstrate that global seawater $^{87}\text{Sr}/^{86}\text{Sr}$ ratios lowered to ~ 0.7070 immediately after the Marinoan glaciation, though values of 0.7075–0.7080 are typical of the Easdale Subgroup interval.

If a Marinoan affiliation of the Port Askaig Formation were to be accepted, this has implications for the wider correlation of Dalradian stratigraphy and understanding of the Proterozoic evolution of the Laurentian margin. The Sturtian glaciation would not be represented in the Dalradian sequence, apart from possibly the Kinlochlaggan Boulder Bed and a pair of negative $\delta^{13}\text{C}$ excursions that could bracket this event. Critical to this scenario is accurate dating of the Appin Group and this must be a high priority. Thus, the comment made by Rooney et al. (2014) continues to apply: "additional tests of regional correlations and geochronological constraints are necessary to more fully resolve the complexities of the Dalradian Supergroup". Fairchild et al. (2018) recommend designation of a Port Askaig Formation exposure in SW Scotland as a Global Boundary Stratotype Section and Point for the Tonian-Cryogenian System boundary (Shields-Zhou et al., 2016), while acknowledging that radiometric constraints or stratigraphically significant biotas or biomarkers are absent. Before this designation is accepted, it is critically important to establish whether the formation represents the Sturtian glaciation or the Marinoan glaciation.

There are several Scottish Dalradian formations that had shale/mudstone protoliths and/or contain syngenetic organic carbon (graphite) or pyrite, and are therefore potentially suitable for Re-Os dating methods. These include the Blair Atholl Subgroup Cuil Bay Slate (Fig. 2a) or its equivalent in Islay, the Bharradail Phyllite, and the Mullagh Dubh Phyllite on Kintyre in SW Scotland (Stephenson et al., 1995). In the central to NE Grampian Highlands, the upper part of the Blair Atholl Subgroup includes metapelite formations such as the Gleann Beag Schist and Glenfiddich Pelite (Stephenson et al., 1995). Further potentially datable Argyll Group formations include the Killiecrankie Schist which locally contains graphitic schists and underlies the Carn Mairg Quartzite in the central Grampians (Fig. 2b), and the aforementioned, stratigraphically higher, Ben Callum Quartzite Formation. The latter contains disseminated pyrite in stratabound mineralization at two horizons (Stephenson et al., 1995; Hill et al., 2015): this pyrite is likely to be syngenetic or syn-diagenetic in origin and to have retained Re-Os characteristics through regional metamorphism. Dating of these formations, and of stratigraphically comparable formations in NW Ireland, is a high priority in order to improve confidence in global chemostratigraphic correlations of the Dalradian Supergroup.

6. Conclusions

The close similarity of the Aberfeldy pyrite Re-Os dates to radiometric age estimates for the stratigraphically overlying formations (the

Tayvallich Volcanics: Dempster et al., 2002) supports the view that the pyrite Re-Os system has survived amphibolite-facies regional metamorphism and that the date represents the depositional timing of sedimentation of the protoliths of the Ben Eagach Schist–Easdale Slate formations. Pyrite samples from the two stratiform barite deposits yield similar Re-Os dates and initial $^{187}\text{Os}/^{188}\text{Os}$ ratios which support other evidence for a syngenetic and/or syn-early-diagenetic depositional model for mineralization. The relatively uniform ratios for initial Os isotopes in pyrite, in conjunction with previous Sr isotope data, attest to large volumes of metalliferous formation waters derived from the underlying sediment pile and/or continental basement. Venting of these fluids would be less likely if the underlying formations had previously been metamorphosed. Incorporation into the Ben Eagach Schist of reworked sands derived from the underlying Cairn Maig Quartzite Formation also implies that the underlying strata had not been metamorphosed. In combination, this evidence supports a hypothesis that sedimentation was continuous throughout the Argyll Group and into the overlying Southern Highland Group, at least in the central Grampian Highlands.

Our dating adds further uncertainties to the chronostratigraphic correlation of the lower Argyll Group sequence and its basal diamictite, the Port Askaig Formation. Accurate dating of this sequence is essential in order to provide confidence in the global correlation of chemostratigraphic features in the Dalradian Supergroup, particularly given recent proposals (Fairchild et al., 2018) that diamictite exposures in the Garvellach Islands (Islay, SW Scotland) should be designated a Global Boundary Stratotype Section and Point for the Tonian-Cryogenian boundary.

CRedit authorship contribution statement

N.R. Moles: Conceptualization, Data curation, Funding acquisition, Investigation, Writing – review & editing, Methodology, Validation. **D. Selby:** Conceptualization, Data curation, Funding acquisition, Investigation, Writing – review & editing.

Declaration of Competing Interest

The authors declare that they have no known competing financial interests or personal relationships that could have appeared to influence the work reported in this paper.

Data availability

Data will be made available on request.

Acknowledgements

We thank Owen Dickinson and Ian Hughes of M-I Drilling Fluids UK Ltd. and Dr Rachael Bullock for assistance with sample collection. DS acknowledges technical support from Geoff Nowell, Antonia Hoffman and Chris Ottley. NM thanks the University of Brighton School of Applied Sciences for technical support and part-funding of the Duntanlich Re-Os analyses, and the Scottish Universities Environmental Research Centre (SUERC) for sulfur isotope analyses. The Editor and anonymous reviewers are thanked for their many suggestions that helped to improve the manuscript.

References

- Alsop, G.I., Prave, A.R., Condon, D.J., Phillips, C.A., 2000. Cleaved clasts in Dalradian conglomerates: possible evidence for Neoproterozoic compressional tectonism in Scotland and Ireland? *Geol. J.* 35, 87–90.
- Anderton, R., 1985. Sedimentation and tectonics in the Scottish Dalradian. *Scott. J. Geol.* 21, 407–436.
- BGS/ODPM, 2006. *Minerals planning factsheet – Barytes*. British Geological Survey & Office of the Deputy Prime Minister, 5 pp.
- Brasier, M.D., Shields, G., 2000. Neoproterozoic chemostratigraphy and correlation of the Port Askaig glaciation, Dalradian Supergroup of Scotland. *J. Geol. Soc. Lond.* 157, 909–914.
- Brenan, J.M., Cherniak, D.J., Rose, L.A., 2000. Diffusion of osmium in pyrrhotite and pyrite: Implications for closure of the Re-Os isotopic system. *Earth and Planetary Science Letters* 180, 399–413.
- Brennan, D.T., Pearson, D.M., Link, P.K., Chamberlain, K.R., 2020. Neoproterozoic Windermere Supergroup near Bayhorse, Idaho: late-stage Rodinian rifting was deflected west around the Belt basin. *Tectonics* 39 (8). <https://doi.org/10.1029/2020TC006145>.
- Chew, D.M., Fallon, N., Kennelly, C., Quentin Crowley, Q., Pointon, M., 2009. Basic volcanism contemporaneous with the Sturtian glacial episode in NE Scotland. *Earth Environ. Sci. Trans. R. Soc. Edinb.* 100, 399–415.
- Coats, J.S., Smith, C.G., Fortey, N.J., Gallagher, M.J., May, F., McCourt, W.J., 1980. Stratabound barium-zinc mineralization in Dalradian Schist near Aberfeldy, Scotland. *Transactions Institute of Mining and Metallurgy* 89, B110–B122.
- Coats, J.S., Smith, C.G., Gallagher, M.J., May, F., McCourt, W.J., Parker, M.E., Fortey, N.J., 1981. Stratabound barium-zinc mineralization in Dalradian Schist near Aberfeldy. Final report. Institute of Geological Sciences Mineral Reconnaissance Programme Report no. Scotland, p. 40.
- Cox, G.M., Halverson, G.P., Stevenson, R.K., Vokaty, M., Poirier, A., Kunzmann, M., Li, Z.-X., Denysyn, S.W., Strauss, J.V., Macdonald, F.A., 2016. Continental flood basalt weathering as a trigger for Neoproterozoic Snowball Earth. *Earth Planet. Sci. Lett.* 446, 89–99.
- Cumming, V.M., Poulton, S.W., Rooney, A.D., Selby, D., 2013. Anoxia in the terrestrial environment during the Late Mesoproterozoic. *Geology* 41, 583–586.
- Dalziel, I.W.D., 1991. Pacific margins of Laurentia and East Antarctica-Australia as a conjugate rift pair: evidence and implications for an Eocambrian supercontinent. *Geology* 19, 598–601.
- Dalziel, I.W.D., Soper, N.J., 2001. Neoproterozoic extension on the Scottish Promontory of Laurentia: paleogeographic and tectonic implications. *J. Geol.* 109, 299–317.
- Dempster, T.J., 1985. Uplift patterns and orogenic evolution in the Scottish Dalradian. *J. Geol. Soc. Lond.* 142, 111–128.
- Dempster, T.J., Jess, S.A., 2015. Ikaite pseudomorphs in Neoproterozoic Dalradian slates record Earth's coldest metamorphism. *J. Geol. Soc. Lond.* 172, 459–464.
- Dempster, T.J., Rogers, G., Tanner, P.W.G., Bluck, B.J., Muir, R.J., Redwood, S.D., Ireland, T.R., Paterson, B.A., 2002. Timing of deposition, orogenesis and glaciation within the Dalradian rocks of Scotland: Constraints from U-Pb zircon ages. *J. Geol. Soc. Lond.* 159, 83–94.
- Emsbo, P., Seal, R.R., Breit, G.N., Diehl, S.F., Shah, A.K., 2016. *Sedimentary exhalative (sedex) zinc-lead-silver deposit model*. U.S. Geological Survey Scientific Investigations Report 2010-5070-N, 57 pp.
- Evans, R.H.S., Tanner, P.W.G., 1996. A late Vendian age for the Kinlochlaggan Boulder Bed (Dalradian)? *J. Geol. Soc. Lond.* 153, 823–826.
- Fairchild, I.J., Spencer, A.M., Ali, D.O., Anderson, R.P., Anderton, R., Boomer, I., Dove, D., Evans, J.D., Hambrey, M.J., Howe, J., Sawaki, Y., Shields, G.A., Skelton, A., Tucker, M.E., Wang, Z., Zhou, Y., 2018. Tonian-Cryogenian boundary sections of Argyll, Scotland. *Precamb. Res.* 19, 37–64.
- Fernandes, N.A., Gleeson, S.A., Magnall, J.M., Creaser, R.A., Martel, E., Fischer, B.J., Sharp, R., 2017. The origin of Late Devonian (Frasnian) stratiform and stratabound mudstone-hosted barite in the Selwyn Basin, Northwest Territories, Canada. *Mar. Pet. Geol.* 85, 1–15.
- Fettes, D.J., Macdonald, R., Fitton, J.G., Stephenson, D., Cooper, M.R., 2011. Geochemical evolution of Dalradian metavolcanic rocks: implications for the breakup of the Rodinia supercontinent. *J. Geol. Soc. Lond.* 168, 1133–1146.
- Fortey, N.J., Beddoe-Stephens, B., 1982. Barium silicates in stratabound Ba-Zn mineralization in the Scottish Dalradian. *Mineral. Mag.* 46, 63–72.
- Fortey, N.J., Smith, C.G., 1986. Stratabound mineralisation in Dalradian rocks near Tyndrum, Perthshire. *Scott. J. Geol.* 22, 377–393.
- Gallagher, M.J., Smith, C.G., Coats, J.S., Greenwood, P.G., Chacksfield, B.J., Fortey, N.J., Nancarrow, P.H.A., 1989. Stratabound barium and base-metal mineralisation in Middle Dalradian metasediments near Braemar, Scotland. British Geological Survey Technical Report WF/89/12 (BGS Mineral Reconnaissance Programme Report 104), 24 pp.
- Goodfellow, W.D., Lydon, J.W., 2007. Sedimentary exhalative (SEDEX) deposits. Geological Association of Canada, Mineral Deposits Division, Special Publication 5, 163–183.
- Gregory, D.D., Large, R.R., Halpin, J.A., Baturina, E.L., Lyons, T.W., Wu, S., Danyushevsky, L., Sack, P.J., Chappaz, A., Maslennikov, V.V., Bull, S.W., 2015. Trace element content of sedimentary pyrite in black shales. *Econ. Geol.* 110, 1389–1410.
- Hall, A.J., 1993. Stratiform mineralization in the Dalradian of Scotland. In: Patrick, R.A. D., Polya, D.A. (Eds.), *Mineralization in the British Isles*. Chapman and Hall, London, pp. 38–101.
- Hall, A.J., Boyce, A.J., Fallick, A.E., 1988. A sulphur isotope study of iron sulphides in the Late Precambrian Dalradian Easdale Slate Formation, Argyll, Scotland. *Mineral. Mag.* 52, 483–490.
- Hall, A.J., Boyce, A.J., Fallick, A.E., Hamilton, P.J., 1991. Isotopic evidence of the depositional environment of Late Proterozoic stratiform mineralisation, Aberfeldy, Scotland. *Chemical Geology (Isotope Geoscience Section)* 87, 99–114.
- Hall, A.J., Boyce, A.J., Fallick, A.E., 1994. A sulphur isotope study of iron sulphides in the late Precambrian Dalradian Ardrishaig Phyllite Formation, Knapdale, Argyll. *Scott. J. Geol.* 30, 63–71.
- Halliday, A.N., Graham, C.M., Aftalion, M., Dymoke, P., 1989. The depositional age of the Dalradian Supergroup: U-Pb and Sm-Nd isotopic studies of the Tayvallich Volcanics, Scotland. *J. Geol. Soc. Lond.* 146, 3–6.

- Halverson, G.P., Dudás, F.Ö., Maloof, A.C., Bowring, S.A., 2017. Evolution of the $^{87}\text{Sr}/^{86}\text{Sr}$ composition of Neoproterozoic seawater. *Palaeogeogr. Palaeoclimatol. Palaeoecol.* 256, 103–129.
- Halverson, G.P., Porter, S.M., Shields, G.A., 2020. Chapter 17: The Tonian and Cryogenian Periods. In: Gradstein, F.M., Ogg, J.G., Schmitz, M.D., Ogg, G.M. (Eds.), *Geologic Time Scale 2020*, Volume 1. Elsevier.
- Harris, A.L., Haselock, P.J., Kennedy, M., Mendrum, J.R., 1994. The Dalradian Supergroup in Scotland, Shetland and Ireland. In: Gibbons, W., Harris, A.L. (eds) *A revised correlation of Precambrian rocks in British Isles*. Geological Society, London, Special Report 22, 33–53.
- Hayward, N., Magnall, J.M., Taylor, M., King, R., McMillan, N., Gleeson, S.A., 2021. The Teena Zn-Pb deposit (McArthur Basin, Australia). Part I: Syndiagenetic base metal sulfide mineralization related to dynamic subsalin evolution. *Econ. Geol.* 116, 1743–1768.
- Hill, N.J., Jenkin, G.R.T., Boyce, A.J., Sangster, C.J.S., Catterall, D.J., Holwell, D.A., Nadem, J., Rice, C.M., 2015. How the Neoproterozoic S-isotope record illuminates the genesis of vein gold systems: an example from the Dalradian Supergroup in Scotland. In: Jenkin, G.R.T., Lusty, P.A.J., McDonald, I., Smith, M.P., Boyce, A.J., Wilkinson, J.J. (eds) *Ore Deposits in an Evolving Earth*. Geological Society, London, Special Publications 393, 213–247.
- Hnatyshin, D., Creaser, R.A., Meffre, S., Stern, R.A., Wilkinson, J.D., Turner, E.C., 2020. Understanding the microscale spatial distribution and mineralogical residency of Re in pyrite: Examples from carbonate-hosted Zn-Pb ores and implications for pyrite Re-Os geochronology. *Chem. Geol.* 533, 119427.
- Hoffman, P.F., Abbot, D.S., Ashkenazy, Y., Benn, D.L., Brocks, J.J., Cohen, P.A., Cox, G. M., Creveling, J.R., Donnadieu, Y., Erwin, D.H., Fairchild, I.J., Ferreira, D., Goodman, J.C., Halverson, G.P., Jansen, M.F., LeHir, G., Love, G.D., Macdonald, F. A., Maloof, A.C., Partin, C.A., Ramstein, G., Rose, B.E.J., Rose, C.V., Sadler, P.M., Tziperman, E., Voigt, A., Warren, S.G., 2017. Snowball Earth climate dynamics and Cryogenian geology-geobiology. *Sci. Adv.* 3, e1600983.
- Hutton, D.H.W., Alsop, G.I., 2004. Evidence for a major Neoproterozoic orogenic unconformity within the Dalradian Supergroup of NW Ireland. *J. Geol. Soc. Lond.* 161, 629–640.
- Hutton, D.H.W., Alsop, G.I., 2005. Reply to Discussion on 'Evidence for a major Neoproterozoic orogenic unconformity within the Dalradian Supergroup of NW Ireland'. *J. Geol. Soc. Lond.* 162, 221–224.
- Kelley, K.D., Leach, D.L., Johnson, C.A., Clark, J.L., Fayek, M., Slack, J.F., Anderson, V. M., Ayuso, R.A., Ridley, W.L., 2004. Textural, compositional, and sulfur isotope variations of sulfide minerals in the Red Dog Sn-Pb-Ag deposits: Implications for ore formation. *Econ. Geol.* 99, 1509–1532.
- Kemp, D.B., Fraser, W.T., Izumi, K., 2018. Stratigraphic completeness and resolution in an ancient mudrock succession. *Sedimentology* 65, 1875–1890.
- Leach, D.L., Sangster, D.F., Kelley, K.D., Large, R.R., Garven, G., Allen, C.R., Gutzmer, J., Walters, S., 2005. Sediment-hosted lead-zinc deposits: A global perspective. *Econ. Geol.* 100th Anniversary Volume, 561–607.
- Leach, D.L., Bradley, D.C., Huston, D., Pisarevsky, S.A., Taylor, R.D., Gardoll, J., 2010. Sediment-hosted lead-zinc deposits in Earth history. *Econ. Geol.* 105, 593–625.
- Li, Y., Vermeesch, P., 2021. Short communication: Inverse isochron regression for Re-Os, K-Ca and other chronometers. *Geochronology* 3, 415–420. <https://doi.org/10.5194/gchron-3-415-2021>.
- Li, Y., Selby, D., Li, X.-H., Ottley, C.J., 2018a. Multisourced metals enriched by magmatic-hydrothermal fluids in stratabound deposits of the Middle-Lower Yangtze River metallogenic belt, China. *Geology* 46, 391–394.
- Li, Y., Zhang, S., Hobbs, R., Caiado, C., Sproson, A.D., Selby, D., Rooney, A.D., 2018b. Monte Carlo sampling for error propagation in linear regression and applications in isochron geochronology. *Science Bulletin* 64, 189–197.
- Ludwig, K.R., 1980. Calculation of uncertainties of U-Pb isotope data. *Earth and Planetary Science Letters* 46, 212–220.
- Ludwig, K., 2011. Isoplot, Version 4.15: *A Geochronology Toolkit for Microsoft Excel*. Berkeley Geochronology Centre Special. Publication 4.
- Magnall, J.M., Gleeson, S.A., Paradis, S., 2020. A new sub-seafloor replacement model for the Macmillan Pass clastic-dominant Zn-Pb ± Ba deposits (Yukon, Canada). *Econ. Geol.* 115, 953–959.
- Manoel, T.N., Selby, D., Galvez, M.E., Leite, J.A.D., Figueiredo, L.N., 2021. A pre-Sturtian depositional age of the lower Paraguay Belt, Western Brazil, and its relationship to western Gondwana magmatism. *Gondw. Res.* 89, 238–246.
- McCay, G.A., Prave, A.R., Alsop, G.I., Fallick, A.E., 2006. A Glacial Trinity: Neoproterozoic Earth history within the British – Irish Caledonides. *Geology* 34, 909–912.
- M-I SWACO, 2014. *Duntanlich Mine Plan*. Presentation prepared by Dalgleish Associates Limited, Dunblane, Scotland.
- Miall, A.D., 2014. The emptiness of the stratigraphic record: A preliminary evaluation of missing time in the Mesaverde Group, Book Cliffs, Utah, U.S.A. *J. Sediment. Res.* 84, 457–469.
- Moles, N.R., 1983. Sphalerite composition in relation to deposition and metamorphism of the Foss stratiform Ba-Zn-Pb deposit, Aberfeldy, Scotland. *Mineral. Mag.* 47, 487–500.
- Moles, N.R., 1985a. Metamorphic conditions and uplift history in central Perthshire: evidence from mineral equilibria in the Foss celsian-barite-sulphide deposit, Aberfeldy. *J. Geol. Soc. Lond.* 142, 39–52.
- Moles, N.R., 1985b. Geology, geochemistry and petrology of the Foss stratiform barite – base metal deposit and adjacent Dalradian metasediments, near Aberfeldy, Scotland. University of Edinburgh. PhD thesis.
- Moles, N.R., Boyce, A.J., 2019. Neoproterozoic microbial processes in chemical sediment diagenesis: evidence from the Aberfeldy barite deposits (extended abstract, oral presentation). Life with Ore Deposits on Earth – 15th SGA Biennial Meeting 2019. *Proceedings* 4, 1413–1416.
- Moles, N.R., Boyce, A.J., Fallick, A.E., 2015. Abundant sulphate in the Neoproterozoic ocean: implications of constant $\delta^{34}\text{S}$ of barite in the Aberfeldy SEDEX deposits, Scottish Dalradian. In: Jenkin, G.R.T., Lusty, P.A.J., McDonald, I., Smith, M.P., Boyce, A.J., Wilkinson, J.J. (eds), *Ore deposits in an evolving Earth*. Geological Society of London, Special Publications 393, 189–212. DOI: 10.1144/SP393.7.
- Moles, N.R., Boyce, A.J., Selby, D., Warke, M.R., Gregory, B., and Claire, M.W., 2020. Global seawater sulfate isotope composition and atmospheric-biospheric evolution constrained at 605 Ma by pyrite Re-Os dating and $\delta^{34}\text{S}$, $\delta^{18}\text{O}$ and $\Delta^{17}\text{O}$ analyses of the Aberfeldy stratiform barite deposits, Scotland (abstract, oral presentation). Sulfur in the Earth system: From microbes to global cycles through Earth history. Geological Society of London virtual conference, 16-17 November 2020, p.32.
- Mukherjee, I., Large, R., 2017. Application of pyrite trace element chemistry to exploration for SEDEX style Zn-Pb deposits: McArthur Basin, Northern Territory, Australia. *Ore Geol. Rev.* 81, 1249–1270.
- Muller, E., Philippot, P., Rollion-Bard, C., Cartigny, P., Assayag, N., Marin-Carbonne, J., Mohan, M.R., Sarma, D.S., 2017. Primary sulfur isotope signatures preserved in high-grade Archean barite deposits of the Sargur Group, Dharwar Craton, India. *Precamb. Res.* 295, 38–47.
- Nadoll, P., Angerer, T., Mauk, J.L., French, D., Walshe, J., 2014. The chemistry of hydrothermal magnetite: a review. *Ore Geol. Rev.* 61, 1–32.
- Noble, S.R., Hyslop, E.K., Highton, A.J., 1996. High precision U-Pb monazite geochronology of the c. 806 Ma Grampian Slide and the implications for the evolution of the Central Highlands. *J. Geol. Soc. Lond.* 153, 511–514.
- Paradis, S., Hnatyshin, D., Simandl, G.L., Creaser, R.A., 2020. Re-Os pyrite geochronology of the Yellowhead-type mineralization, Pend Oreille Mine, Kootenay Arc, Metaline District, Washington. *Econ. Geol.* 115, 1373–1384.
- Parnell, J., Perez, M., Armstrong, J., Bullock, L., Feldmann, J., Boyce, A.J., 2017. A black shale protolith for gold-tellurium mineralisation in the Dalradian Supergroup (Neoproterozoic) of Britain and Ireland. *Appl. Earth Sci.* 126, 161–175.
- Pidgeon, R.T., Compston, W., 1992. A SHRIMP ion microprobe study of inherited and magmatic zircons from four Scottish Caledonian granites. *Earth Environ. Sci. Trans. R. Soc. Edinb.* 83, 473–483.
- Pitcher, W.S., Berger, A.R., 1972. *The geology of Donegal: a study of granite emplacement and unroofing*. Wiley Interscience, New York, p. 435.
- Prave, A.R., Fallick, A.E., 2011. The Neoproterozoic glaciogenic deposits of Scotland and Ireland. In: Arnaud, E., Halverson, G.P., Shields-Zhou, G. (eds) Chapter 63, *The Geological Record of Neoproterozoic Glaciations*. Geological Society, London, Memoirs 36, 643–648.
- Prave, A.R., Fallick, A.E., Thomas, C.W., Graham, C.M., 2009a. A composite C-isotope profile for the Neoproterozoic Dalradian Supergroup of Scotland and Ireland. *J. Geol. Soc. Lond.* 166, 845–857.
- Prave, A.R., Strachan, R.A., Fallick, A.E., 2009b. Global C cycle perturbations recorded in marbles: a record of Neoproterozoic Earth history within the Dalradian succession of the Shetland Islands, Scotland. *J. Geol. Soc. Lond.* 166, 129–135.
- Pringle, J., 1940. The discovery of Cambrian trilobites in the Highland Border rocks near Callander, Perthshire (Scotland). *The Advancement of Science* 1, 252.
- Provov, A.W., Newell, D.L., Dehler, C.M., Ault, A.K., Yonkee, W.A., Thomson, S.N., Mahan, K.H., 2021. Revised maximum depositional age for the Ediacaran Browns Hole Formation; implications for western Laurentia Neoproterozoic stratigraphy. *Lithosphere* article 1757114, 14 pages. <https://doi.org/10.2113/2021/1757114>.
- Rajabi, A., Alfonso, P., Canet, C., Rastad, E., Niroomand, S., Modabberli, S., Mahmoodi, P., 2020. The world-class Koushk Zn-Pb deposit, Central Iran: A genetic model for vent-proximal shale-hosted massive sulfide (SHMS) deposits - based on paragenesis and stable isotope geochemistry. *Ore Geol. Rev.* 124, 103654.
- Reynolds, N., McArdle, P., Pyne, J.F., Farrell, L.P.C., Flegg, A.M., 1990. *Mineral localities in the Dalradian and associated igneous rocks of Connemara, County Galway*. Geological Survey of Ireland. Report Series RS 90/2.
- Reynolds, M.A., Gleeson, S.A., Creaser, R.A., Friedlander, B.A., Haywood, J.C., Hnatyshin, D., McCusker, J., Waldron, J.W.F., 2021. Diagenetic controls on the formation of the Anarraq Clastic-Dominated Zn-Pb-Ag deposit, Red Dog District, Alaska. *Econ. Geol.* 116, 1803–1824.
- Rogers, G., Dempster, T.J., Bluck, B.J., Tanner, P.W.G., 1989. A high precision U-Pb age for the Ben Vuirich Granite: implications for the evolution of the Scottish Dalradian Supergroup. *J. Geol. Soc. Lond.* 146, 789–798.
- Rooney, A.D., Chew, D.M., Selby, D., 2011. Re-Os geochronology of the Neoproterozoic-Cambrian Dalradian Supergroup of Scotland and Ireland: Implications for Neoproterozoic stratigraphy, glaciations and Re-Os systematics. *Precamb. Res.* 185, 202–214.
- Rooney, A.D., Cantine, M.D., Bergmann, K.D., Gómez-Pérez, I., Al Baloushi, B., Boag, T. H., Busch, J.F., Sperling, E.A., Strauss, V., 2020. Calibrating the coevolution of Ediacaran life and environment. *PNAS* 117, 16824–16830.
- Rooney, A.D., Macdonald, F., Strauss, J.V., Dudás, F.Ö., Hallmann, C., Selby, D., 2014. Re-Os geochronology and coupled Os-Sr isotope constraints on the Sturtian snowball Earth. *Proceedings of the National Academy of Sciences of the United States of America* 111, 51–56.
- Rose, C.V., Swanson-Hysell, N.L., Husson, J.M., Poppick, L.N., Cottle, J.M., Schoene, B., Maloof, A.C., 2012. Constraints on the origin and relative timing of the Trezona $\delta^{13}\text{C}$ anomaly below the end-Cryogenian glaciation. *Earth Planet. Sci. Lett.* 319–320, 241–250.
- Ruffell, A.H., Moles, N.R., Parnell, J., 1998. Characterisation and prediction of sediment-hosted ore deposits using sequence stratigraphy. *Ore Geol. Rev.* 12, 207–223.
- Russell, M.J., 1985. The evolution of the Scottish mineral sub-province. *Scott. J. Geol.* 21, 513–545.

- Sadler, P.M., 1981. Sedimentation rates and the completeness of stratigraphic sections. *J. Geol.* 89, 569–584.
- Sawaki, Y., Kawai, T., Shibuya, T., Tahata, M., Omori, S., Komiya, T., Yoshida, N., Hirata, T., Ohno, T., Windley, B.F., Maruyama, S., 2010. $^{87}\text{Sr}/^{86}\text{Sr}$ chemostratigraphy of Neoproterozoic Dalradian carbonates below the Port Askaig Glaciogenic Formation, Scotland. *Precamb. Res.* 179, 150–164.
- Selby, D., Creaser, R.A., 2003. Re-Os geochronology of organic-rich sediments: An evaluation of organic matter analysis methods. *Chem. Geol.* 200, 225–240.
- Selby, D., Kelley, K.D., Hitzman, M.W., Zieg, J., 2009. Re-Os sulfide (bornite, chalcopyrite, and pyrite) systematics of the carbonate-hosted copper deposits at Ruby Creek, southern Brooks Range, Alaska. *Econ. Geol.* 104, 437–444.
- Shields, G.A. et al. (36 authors), 2021. A template for an improved rock-based subdivision of the pre-Cryogenian timescale. *Journal of the Geological Society, London*, 179. <https://doi.org/10.1144/jgs2020-222>.
- Shields, G.A., Veizer, J., 2002. Precambrian marine carbonate isotope database: Version 1.1. *Geochem. Geophys. Geosyst.* 3, 1–12.
- Shields-Zhou, G.A., Porter, S.M., Halverson, G.P., 2016. A new rock-based definition for the Cryogenian Period (circa 720–635 Ma). *Episodes* 39, 3–8.
- Smoliar, M.I., Walker, R.J., Morgan, J.W., 1996. Re-Os ages of group IIA, IIIA, IVA, and IVB iron meteorites. *Science* 271, 1099–1102.
- Stephenson, D., Gould, D., Clark, G.C., Fettes, D.J., Fletcher, T.P., Gallagher, M.J., Johnstone, G.S., Key, R.M., Mallick, D.I.J., Mendum, J.R., Merritt, J.R., Musson, R.M. W., Mykura, W., Peacock, J.D., Smith, D.I., 1995. *British Regional Geology: The Grampian Highlands*, 4th edition. HMSO for the British Geological Survey, London.
- Stephenson, D., Mendum, J.R., Fettes, D.J., Leslie, A.G., 2013. The Dalradian rocks of Scotland: an introduction. *Proceedings of the Geologists' Association* 124, 3–82.
- Strachan, R.A., Harris, A.L., Fettes, D.J., Smith, M., 2002. The Northern Highland and Grampian terranes. In: Trewin, N.H. (Ed.), *The Geology of Scotland*, 4th edition. The Geological Society, London, pp. 81–148.
- Sturt, B.A., 1961. The geological structure of the area south of Loch Tummel. *Q. J. Geol. Soc. Lond.* 117, 131–156.
- Swenson, D.H., Laux, S.J., Burns, A.R., Perley, P.C., Boast, A.M., 1981. The Foss barite deposit, Aberfeldy, Scotland: depositional and structural history of a Dalradian strata-bound orebody (abstract). *Trans. Inst. Min. Metall.* 90, B57.
- Tanner, P.W.G., 1995. New evidence that the Lower Cambrian Leny Limestone at Callander, Perthshire, belongs to the Dalradian Supergroup, and a re-assessment of the 'exotic' status of the Highland Border Complex. *Geol. Mag.* 132, 473–483.
- Tanner, P.W.G., 2005. Discussion on 'Evidence for a major Neoproterozoic orogenic unconformity within the Dalradian Supergroup of NW Ireland'. *J. Geol. Soc. Lond.* 162, 221–224.
- Tanner, P.W.G., Leslie, A.G., Gillespie, M.R., 2006. Structural setting and petrogenesis of a rift-related intrusion: the Ben Vuirich Granite of the Grampian Highlands, Scotland. *Scott. J. Geol.* 42, 113–136.
- Thomas, C.W., Graham, C.M., Ellam, R.M., Fallick, A.E., 2004. $^{87}\text{Sr}/^{86}\text{Sr}$ chemostratigraphy of Neoproterozoic Dalradian limestones of Scotland and Ireland: constraints on depositional ages and time scales. *J. Geol. Soc. Lond.* 161, 229–242.
- Toma, J., Creaser, R.A., Card, C., Stern, R.A., Chacko, T., Steele-MacInnis, M., 2022. Re-Os systematics and chronology of graphite. *Geochim. Cosmochim. Acta* 323, 164–182.
- Torsvik, T.H., Lohmann, L.K.C. Sturt, B.A., 1995. Vendian glaciations and their relation to the dispersal of Rodinia: paleomagnetic constraints. *Geology* 23, 727–730.
- Treagus, J.E., 1969. The Kinlochlaggan Boulder Bed. *Proceedings of the Geological Society, London* 1654, 55–60.
- Treagus, J.E., 1981. The Lower Dalradian Kinlochlaggan Boulder Bed, central Scotland. In: Hambrey, M.J., Harland, W.B. (Eds.), *Earth's Pre-Pleistocene Glacial Record*. Cambridge University Press, Cambridge, pp. 637–639.
- Treagus, J.E., Tanner, P.W.G., Thomas, P.R., Scott, R.A., Stephenson, D., 2013. The Dalradian rocks of the central Grampian Highlands of Scotland. *Proc. Geol. Assoc.* 124, 148–214.
- Treagus, J.E., 2000. *The Solid Geology of the Schiehallion District*. British Geological Survey, Edinburgh, Memoirs (Sheet 55W).
- van Acken, D., Su, W., Gao, J., Creaser, R.A., 2014. Preservation of Re-Os isotope signatures in pyrite throughout low-T, high-P eclogite facies metamorphism. *Terra Nova* 26, 402–407.
- Veizer, J., 1989. Strontium isotopes in seawater through time. *Annu. Rev. Earth Planet. Sci.* 17, 141–167.
- Vermeesch, P., 2018. IsoplotR: A free and open toolbox for geochronology. *Geosci. Front.* 9, 1479–1493.
- Vernon, R., Holdsworth, R.E., Selby, D., Dempsey, E.D., Finlay, A., Fallick, A.E., 2014. Structural characteristics and Re-Os dating of quartz-pyrite veins in the Lewisian Gneiss Complex, NW Scotland: Evidence of an Early Paleoproterozoic hydrothermal regime during terrane amalgamation. *Precamb. Res.* 246, 256–267.
- Walters, J.B., Cruz-Urbe, A.M., Marshall, H.R., 2019. Isotopic compositions of sulfides in exhumed high-pressure terranes: Implications for sulfur cycling in subduction zones. *Geochem. Geophys. Geosyst.* 20, 3347–3374.
- Willan, R.C.R., 1981. Geochemistry of host rocks to the Aberfeldy barite deposit, Scotland (abstract). *Trans. Inst. Min. Metall.* 90, B57.
- Woodcock, N.H., 2004. Life span and fate of basins. *Geology* 32, 685–688.
- Yang, C., Li, Y., Selby, D., Wan, B., Guan, C., Zhou, C., Li, X.-H., 2022. Implications for Ediacaran biological evolution from the ca. 602 Ma Lantian biota in China. *Geology*. <https://doi.org/10.1130/G49734.1>.
- Yonkee, W.A., Dehler, C.D., Link, P.K., Balgord, E.A., Keeley, J.A., Hayes, D.S., Wells, M. L., Fanning, C.M., Johnston, S.M., 2014. Tectonostratigraphic framework of Neoproterozoic to Cambrian strata, west-central U.S.: Protracted rifting, glaciation, and evolution of the North American Cordilleran margin. *Earth Sci. Rev.* 136, 59–95.
- Yuan, L., Zhou, Y., Chen, X., Zhu, M., Poulton, S.W., Tian, Z., Li, D., Thirlwall, M., Shields, G.A., 2022. Multiple ocean oxygenation events during the Ediacaran Period: Mo isotope evidence from the Nanhua Basin, South China. *Precambrian Research*. DOI 10.31223/X5RS86.